Fall 2022

Effect of in-situ formed nano-calcite particles on hydration and properties of cement-based materials

Bowen Tan

Department:

EFFECT OF IN-SITU FORMED NANO-CALCITE PARTICLES ON HYDRATION AND PROPERTIES OF CEMENT-BASED MATERIALS

by

BOWEN TAN

A THESIS

Presented to the Graduate Faculty of the

MISSOURI UNIVERSITY OF SCIENCE AND TECHNOLOGY

In Partial Fulfillment of the Requirements for the Degree

MASTER OF SCIENCE

in

CIVIL ENGINEERING

2022

Approved by:

Hongyan Ma, Advisor

Kamal Khayat

Aditya Kumar

ABSTRACT

The in-situ preparation of nano-calcite via bubbling method and the effects of the nano-calcite on the hydration process and properties of the cement-based materials are investigated in this research. The nano-calcite is synthesized under different conditions and added into Portland cement to prepare test samples. The bubbling method is then introduced in upcycling the municipal solid waste incineration (MSWI) ashes, and the effects of the upcycled MSWI ashes on the hydration of Portland cement is investigated. Experimental results illustrate that the CO_2 bubbling method can produce nanometer-to-sub-micron-sized calcite particles, and the synthesis rate and the morphology of the nano-calcite can be influenced by several factors (e.g., CO_2 flow rate and superplasticizer). The incorporation of nano-calcite has shown a significant, positive effects, that is, increase in the early-stage mechanical properties of the cement pastes. The increase varies with the dosage of the nano-calcite. Treated and untreated MSWI ashes are used as alternative supplementary cementitious materials (ASCMs) to investigate the feasibility of the treatment of MSWI ashes with CO_2 bubbling method. Results indicate that the CO_2 bubbling method can improve the quality of some MSWI ashes as ASCMs. Compared with the untreated MSWI ash paste samples, the compressive strength of the treated-small aggregate (a specific type of MSWI bottom ash) samples has increased by ~100% at 7 days. Though the properties of the treated samples are still not comparable to the plain control groups, this study provides positive evidence on the treatment of MSWI ashes with CO_2, making synchronous CO_2 capture/utilization and MSWI ash upcycling a feasible strategy.

ACKNOWLEDGMENTS

I would like to express my deepest gratitude to my advisor, Dr. Ma, for his patience, motivation, enthusiasm, and immense knowledge. I am extremely grateful for all the supports and inspirations he offered me during my master's study, this study would not have been possible without Dr. Ma.

Very special thanks to Dr. Wenyu Liao, who has been my senior in Dr. Ma's research group, for his relentless help in the lab. From him I learnt almost all of the testing and analyzing methods for my study, and he was always there when I need further support.

Many thanks to all of the members of staff in Missouri S&T. My master's study was rough, but with the help from them, I am finally able to present this thesis and finished my master's study.

Last, but not the least, my warm and heartfelt thanks go to my family for their tremendous support and hope they had given to me. Those hope supported me whenever I needed them.

TABLE OF CONTENTS

Page

LIST OF ILLUSTRATIONS

LIST OF TABLES

1. INTRODUCTION

1.1. BACKGROUND

The atmospheric concentration of carbon dioxide (CO_2), known as a common greenhouse gas, is steadily increasing due to the human activities such as burning fossil fuels, removal of forests and the manufacture of cement [1]. The increasing concentration of greenhouse gases results in the strong greenhouse effect, which leads to the rise of global temperature, changes of the global climate; furthermore, rises the global sea level. Records suggests that the global sea level increased by 15 cm due to the 0.5℃ rising in global temperature during 1900-1993 [2]. The steadily increasing of anthropogenic CO_2 emissions (~0.5%-2% per year) reached a record high of 36.44 billion tones (Gt) per year in 2019; and this will continue in the foreseeable future [3]. The emissions have resulted in an atmospheric CO_2 concentration of 420 ppm in 2021 [4] – the highest level since 3 million years ago [5, 6]. It is noted that there can be a time lag between atmospheric CO_2 concentration increase and the resultant warming effect [7]. That is to say, the projected warming effects corresponding to a >400 ppm CO_2 concentration (e.g., 2-3°C warmer than the pre-industrial age and >6 m higher sea level than present [8]) may emerge in the coming decades. A report from Intergovernmental Panel on Climate Change, the concentration of atmospheric CO_2 will increase to 1200ppm by 2100 if no effective anthropogenic interventions are implemented at scale [9]. In addition, the climate change will also lead to higher risks of extreme weathers and the extinction of some species. A research has estimated a 15-37% extinction of species till 2050, due to the climate change, with the concentration of atmospheric CO_2 around 550ppm [10].

To address the challenges tied to global warming, resolute and vigorous actions are urgently needed to stop and even reverse the rapid increase of atmospheric CO_2 to avoid nonreversible, catastrophic consequences. Facing with this challenge, the White House has set a 2030 target of 50%-52% reduction in emissions vis-à-vis their 2005 levels [11]. This goal is too rigorous to be achieved with the current and emerging incremental technologies [12]. The technological limitations and urgent needs to reduce CO_2 emission/concentration highlight the necessity to develop and implement novel, breakthrough technologies – including carbon capture, utilization and storage (CCUS) in various formats and at various scales – as immediate responses, especially in CO_2-intensive industrial sectors (e.g., cement and concrete production).

1.2. DECARBONIZATION OF CEMENT AND CONCRETE

Cement has been used for 200 years for making concrete, the foundation of modern infrastructure [13]. However, cement production is responsible for ~10% (or >4 Gt/year) of anthropogenic CO_2 emissions [14, 15]. Thus, the cement and concrete industry is under increasing pressure to reduce CO_2 emission, and even to achieve carbon neutrality [16]. An United Nation's report [14] has identified three effective approaches to improve the eco-efficiency of cement: (1) Increasing use of CO_2-efficient supplementary cementitious materials (SCMs); (2) Improving cement efficiency; and (3) Developing sustainable alternative cements.

To date, the most effective strategy to bring eco-efficiency to cement/concrete is to substitute cement partially (up to 70%) with SCMs, which include blast-furnace slag (BFS), fly ash, silica fume, calcined clay, pozzolans, etc. [17]. However, annual

productions of BFS and fly ash – the two major SCMs – are less than 8% and 20% of cement, respectively; and their useful reserves are nearly exhausted [18-21]. The other SCMs are limited by total production, geographical availability, or the need for calcination [22, 23]. This discussion entails that increasing use of SCMs, as an approach to engender eco-efficiency, faces a major challenge of resource shortage [24]. Cement efficiency can also be improved by optimizing aggregate structure[25], and using fillers [26], nanoparticles [27], and chemical admixtures [28]. Broadly speaking, these methods are less effective than using SCMs. Alternative cements, represented by calcium aluminate/sulfoaluminate cements [29, 30], have received market acceptance. These cements can be greener than Portland cement, but they are more expensive due to the need of high-quality raw materials [17]. Alkali-activated materials (AAMs) have garnered attention as cement alternatives [31]. However, they have not been adopted at mass-scale. This is because AAMs require SCMs as raw materials, the availability of which is limited. The needs of costly, alkaline activators (e.g., $NaOH/Na_2SiO_3$; global annual production <10 Mt), and uncertainties in durability, have also prevented widespread adoption of AAMs [32-34]. As discussed above, construction is an ideal beachhead sector for CCUS due to its large market size (e.g., >30 Gt/year concrete) and "permanent" CO_2 storage. The principal hydration products of cement – calcium hydroxide (CH) and calcium-silicate-hydrate (C-S-H) gel – can absorb CO_2 through carbonation[35]. Because of this, CO_2 has been used as a curing agent for cement/ concrete specimens to improve their properties and enhance carbon uptake [36, 37]. However, the requirement of CO_2 penetration into the specimens' interior limits the rate/amount of CO_2 uptake. To overcome this limitation, CarbonCure^{TM} aerates CO_2 into

fresh concrete [38]; however, it allows only ~0.2% CO_2 uptake by weight of cement [39]. Several carbonation-hardening cements (CHCs, a class of alternative cements) have been proposed to absorb CO_2, including cements based on carbonation of CaO/CH (e.g., CarbonBuilt™ [39, 40]), MgO (e.g., Novacem™ [41]), $CaO{\cdot}SiO_2$ (e.g., Solidia™ [42]), and steel slag (e.g., CarbiCrete [43]). CHCs have been advocated to be carbon-efficient, but their net CO_2 uptake is limited by the depth of CO_2 penetration, especially when large structural members are manufactured. These cements also have the following limitations: (1) Scarcity of major precursors (i.e., CaO, MgO, and $CaO{\cdot}SiO_2$) in nature, thus requiring conversion of carbonates for production; (2) Requirement of concentrated CO_2 for carbonation; and (3) Limited to prefabrication of structural members, not cast-in-place construction. These limitations challenge their true CO_2-reduction efficiency.

To sum up, SCMs, higher cement utilization efficiency, and sustainable alternative cements are critical to decarbonize cement and concrete. However, developments of relevant technologies are limited by shortage of resources and/or true CO_2-reduction efficiency. Identifications of new, reliable resources and technologies for developing eco-efficient (e.g., carbon-neutral or even carbon-negative) SCMs and alternative cements represents an urgent need in both industry and academia.

1.3. POTENTIAL RELIABLE RESOURCES

Calcium carbonate ($CaCO_3$) is a common substance usually found in rocks, shells of marine organisms and eggs, it has various polymorphs including calcite, aragonite and vaterite, among those, calcite has the most stable thermodynamic structure [44]. The usage of calcium carbonate has covered multiple areas such as food industry, medical

industry, and construction industry. Majorly the calcium carbonate is used as aggregate in construction materials [45, 46], recently with more research progressed, the calcite has been used in different ways, such as filler material [47, 48], micro fiber [49-52] and early strength agent, for its various scales (macro-, micro- and nano-scale) , morphologies (bulk, granular and fibrous shape), crystal systems (calcite, aragonite, vaterite and amorphous) [53]. Calcium carbonate, in various forms, have been widely considered as a beneficial cement filler in either blended cement (e.g., Type IL cement and Limestone Calcined Clay Cement) or ready-mixed concrete. Since no calcination is needed, ground calcium carbonate (i.e., limestone) can be considered as an eco-efficient cementitious material (filler). In addition, a broad range of industrial solid wastes (e.g., slags, coal ashes, municipal solid waste incineration ashes, and mine tailings) have similar chemical composition with Portland cement. Therefore, these solid wastes – if can be upcycled to obviate their potential negative effects on cement and concrete – will also be eco-efficient cementitious materials (i.e., SCMs).

1.4. THESIS OVERIEW

This work aims to create a novel pathway of improving the eco-efficiency of cement utilization – improving hydration of cement and properties of cement-based materials through *in situ* formed nano calcium carbonate particles in mixing water. It can also be considered as a small-dose functional SCM. This strategy is also modified to upcycle municipal solid waste incineration (MSWI) ashes into SCMs. In such modification, MSWI ashes serve as calcium sources; while the calcium is carbonated into nano calcium carbonate, the residue is dominated by amorphous aluminosilicate. So the

product is a blended SCMs consisting of calcium carbonate nanoparticles and aluminosilicate phases. This thesis has five sections as shown below.

Section 1 is a general introduction to the background and basic rational of the presented studies in this thesis.

Section 2 presents literature reviews regarding synthesis of calcium carbonate nanoparticles and the filler effects of calcium carbonate; and state of the art research about MSWI ashes.

Section 3 encompasses details of the method of *in situ* synthesis of calcium carbonate nanoparticles; parameters affecting the particle size, morphology and polymorph of the formed calcium carbonate nanoparticles; and the effects of the nanoparticles at various dosages on the hydration of cement and strength of cement paste.

Section 4 discusses the potential of MSWI ashes as SCMs of cement concrete; their negative effects; and how the *in situ* CO_2 treatment method could mitigate the negative effects and upcycle the MSWI ashes.

Section 5 summarizes the major conclusions and visions regarding future research (combination of the *in situ* CO_2 treatment and other secondary processing methods to upgrade a broad range of solid wastes into quality SCMs).

2. LITERATURE REVIEW

2.1. THE SYNTHESIS OF NANO-CALCITE AND THE EFFECT OF CALCITE WITH DIFFERENT SIZE ON THE HYDRATION OF CEMENTITIOUS MATERIALS

2.1.1. The Categorization of Calcium Carbonate. Calcium carbonate is an important inorganic chemical filler, it is widely used in polymers, papermaking, coatings, sample glue, chemical building materials, daily chemicals, printing inks, adhesives, and other industries [54-62]. The most common naturally occurring crystal forms of calcium carbonate are calcite, aragonite and vaterite [63], they belong to the trigonal crystal system, the orthorhombic crystal system, and the hexagonal crystal system, respectively. Among the three crystal types, calcite has the most stable structure and mainly exists in marble and limestone, and most natural limestone is formed of calcite [64]. Vaterite, with the least thermodynamic stability, is the least commonly seen polymorph in nature. Vaterite has the highest water solubility, and it is able to transform to calcite and aragonite in aqueous solution quickly [65]. Research suggest that vaterite can transform to aragonite in 60 mins at 60°C, and to calcite in 24 hours in room temperature [66]. The appearance features are spindle and cuboid. Because of the relatively low stability to calcite, aragonite mainly exists in marine sediments and nacre.

Calcium carbonates can be divided into two major groups based on the production methods [67]. Products prepared from calcite, marble, white, shells, limestone and other raw materials through mechanical crushing and ultrafine grinding are called ground calcium carbonate (GCC). GCC has irregular morphology, wide particle size distribution and large particle size. Precipitated calcium carbonate (PCC) is another category of

calcium carbonate that is produced through a series of chemical processes [68]. Generally, PCC and GCC are all formed of calcite, for its stability, except for PCC, the polymorphs can be controlled by changing the reaction conditions [69]. It is used as a filler in products and has a semi-reinforcing function as well as GCC, but with higher purity, better physical properties, smaller particle size and controllable dimension and morphology, PCC is gaining more interest from the researchers and the industries [70] [71]. Though the GCC has advantages in terms of the energy consumption, processing method, cost, particle fluidity and environmental protection [67], the PCC is still gradually taking place of GCC [72]. Besides the mentioned industries that have long been using calcium carbonate as fillers, in other fields, for example, construction materials, the application of limestone is attracting many researchers, especially in recent years [73-77]. From 2000 to 2017, the number of publications per year indexed in Web of Science matching keywords of "concrete and limestone" in search of "Topic" grown from ~50 to ~550 [52].

According to the particle size, the calcium carbonate is divided into three major groups: macro-calcium carbonate, micro-calcium carbonate, and nano-calcium carbonate [78]. There are many studies focus on the effects of calcium carbonate on the properties of cementitious materials, and this review provides an overview of the current studies on the influences of the calcium carbonate on the hydration process, workability, mechanical properties and durability of cementitious materials, along with the commonly used synthesis methods of PCC. Through the summaries of previous references, propose the potential of the application of *in situ* synthesis of nano-calcite and its use in the cementitious materials.

2.1.2. The Synthesis Methods of Nano Calcite. There are three main synthesis systems for nanometer calcium carbonate: Ca^{2+}-H_2O-$CO_3$2- reaction system, Ca^{2+}-R-CO_3^{2-} reaction system, and $Ca(OH)_2$-H_2O-CO_2 reaction system [79-82]. The $Ca(OH)_2$-H_2O-CO_2 reaction system, that is, the carbonization reaction system, uses limestone as the raw material, and is calcined, digested, carbonized, activated, filtered, dried, and crushed to produce active nano-calcium carbonate. By controlling different reaction conditions, calcium carbonate with various shapes such as spherical, cubic, acicular, flaky chain, etc., can be prepared[83]. This system is widely used in industrial synthesis of PCC for its low-cost, high productivity and the ability to control the polymorphs of the calcite [84].

The main synthesis methods of $CaCO_3$ particles are biomimetic synthesis and CO_2 bubbling method [85]. The biomimetic method generally adopts the Ca^{2+}-H_2O-CO_3^{2-} reaction system, Ca^{2+}-R-CO_3^{2-} reaction system, it attempts to mimic the natural conditions of the formation of calcite, trying to control the size and morphology of the calcite particles via the incorporation of organic compounds. The CO_2 bubbling method, which uses the $Ca(OH)_2$-H_2O-CO_2 reaction system, is the main method for industrial production [86].

2.1.3. Biomimetic Synthesis of Calcite. Biomimetic method tries to mimic the natural formation of the calcium carbonates e.g., shells and marine animals which uses the transient amorphous calcium carbonate (ACC) phase to precipitate the crystalline calcium carbonate phases and form structures [87, 88]. By using additives, researchers can have the ability to control the morphologies, polymorphs, and sizes of the products via this method [89]. The experimental conditions for biomimetic synthesis method are

usually mild, makes it easier to implement [82]. The influences of the additives are rather diverse due to the huge amount of possible organic additives that exist. Different types of additives, including surfactants, poly electrolytes, double hydrophilic block copolymers, polysaccharides such as soluble starch, amino acids and organic acids were used as biomimetic agents to achieve different particle morphologies, polymorphs, and sizes [80, 90-96].

There are two main methods for the biomimetic method: precipitation method and reverse emulsion method, and precipitation reaction methods include the spontaneous precipitation and the slow carbonation reaction [85]. Some researchers would also categorize the synthesis methods by the phases of the reactants e.g., the solid-liquid route, liquid-liquid route, and the solid-liquid-gas route [97], and the biomimetic synthesis methods can be categorized as the liquid-liquid route (sometimes solid-liquid route) with Ca^{2+}-H_2O-CO_3^{2-} reaction system, Ca^{2+}-R-CO_3^{2-} reaction system. During the synthesis process, the introduction of additives can have significant influences on the morphology, polymorph and size of $CaCO_3$ particles [85] [80], and both types and the concentrations of the additives can influence the properties of the products. For example, David et al [91], introduced an organic additive named protein TapA to investigate the influences on the formation of calcium carbonate with fast vapor diffusion method. They found that protein TapA can change the morphology of calcium carbonate from rhombohedral to spheric, thus the polymorph was changed from calcite to vaterite, too. Despite of organic additives, other additives: surfactants [98-101], synthetic polymers [102-104], biomolecules [105, 106], amino acids [107, 108], polymer-surfactant mixtures [109-111],

etc. [112, 113], are also proved to have effects on the formation of calcium carbonate crystals.

2.1.3.1. The CO_2 bubbling method. The CO_2 bubbling method is the most commonly used synthesis method of calcium carbonate particles for the industries for its high productivity and low cost. By bubbling CO_2 through $Ca(OH)_2$ (usually in slurries), the $CaCO_3$ particles are formed, the size of the synthesized particles can be easily controlled by controlling the size of the CO_2 bubbles [114-117]. Since $Ca(OH)_2$ can be obtained from limestone and CO_2 is easy to collect from industry flue gas, the cost of this method is relatively low. This method is also gaining more interests for its ability to absorb CO_2, or to catch carbon, in recent years [118-120]. However, the polymorphs of the products are usually limited to cubic or rhombohedral, which is the typical form of calcite phase [114, 117], even with elevated pressure, moderate temperature and additives [121], agglomeration is common for this method [117]. The polymorphs and morphologies of the particles can be altered with the addition of organic additives. Hadiko et al. [95] also achieved the hollow-shaped calcium carbonate particles(calcite and vaterite) with inorganic ions (VO_3^{2-}).

2.1.3.2. Microorganisms and other methods. The microorganisms can help producing calcium carbonate particles, and this is not actually “synthesizing” but “forming” calcium carbonate particles by the microorganisms.

Specific groups of microorganisms are able to induce the formation of calcium carbonate [122], this technology is usually used in the biocement, self-healing concrete and composite biomaterial areas [123]. Microwave assisted methods, ultrasound assisted

methods, alternating current methods, atomized microemulsion methods and spray dying methods are also ways to synthesize calcium carbonate nanoparticles [85].

2.1.4. The Influencing Factors in Synthesizing Calcite. Additives, pH, temperature, Ca^{2+} concentration, reaction time, gas flow rate, and stirring/mixing rate (gas-liquid interfacial area) are all the parameters that can cause differences in the synthesis of calcium carbonate particles [80, 85], some influences induced by additives are already discussed previously. Temperature and pH are usually not considered as influential parameters for the CO_2 bubbling method, for the pH of the initial $Ca(OH)_2$ solution/slurry is usually high: the saturated $Ca(OH)_2$ solution has pH higher than 12. Since the solubility of CO_2 in water decreases with the rise of temperature [124, 125], the CO2 bubbling method is usually performed at relatively low temperature, or room temperature [126]. The solution pH mainly influences the morphology of $CaCO_3$ particles, but not the polymorphs, for the precipitation methods, and the optimized pH range depends on the specific additive that is used [99, 102]. Reaction temperature affects the morphology, polymorph, and the size of precipitated $CaCO_3$ particles. Higher temperature provides sufficient energy for the formation of higher surface energy particles like aragonite and ACC, and with the increasing temperature, the morphology of the particles are elongated, growing on the axile direction [127-129]. Initial concentration of Ca^{2+} affects the size, morphology and polymorph of the $CaCO_3$ particles, for both bubbling method and precipitation methods [85, 130]. In $Ca(OH)_2$ system, lower initial $Ca(OH)_2$ concentration(suspension) results in larger particles, wider particle distributions, and cubic particles, while higher initial concentration results in smaller and irregular shaped particles [131, 132]. However, this does not agree with it in the $CaCl_2$ system,

Yong Sheng Han et al., [133] find out that lower $CaCl_2$ solution produces smaller, spherical particles, and with the increasing concentration, the size is growing, and the shape changes from spherical to rhombic, along with the polymorph changing from the mixture of calcite and vaterite to only calcite. The influences from the reaction time are based on the properties of the $CaCO_3$ polymorphs: for the stability of ACC and aragonite is relatively lower than it of vaterite and calcite, so with the increasing reaction time, the polymorphs are gradually changing from ACC and aragonite to vaterite and calcite [103, 134]. Also the particle size is growing with the increasing reaction time, along with the morphologies getting more regular [103, 108, 135].

2.1.5. Effect of Calcium Carbonate on the Cementitious Materials. Calcium carbonate is usually added into cementitious materials as a typical filler, the major effect is also the filler effect. However, with different particle size, the effect varies, and more effects are introduced when the particle size is lowered into nano-scope. In this part, the effects of calcium carbonate on the cementitious materials are summarized and divided into two major sections by the particle size.

2.1.5.1. Micro-calcium carbonate. Micro-calcium carbonate (1 μm–1 mm), majorly coming from grinding natural limestone into limestone powder or limestone dust, is widely used in producing cementitious materials as a filler, mineral admixture, or sometimes, as supplementary cementitious materials.

By filling up the voids between the aggregate particles, the limestone powder is able to reduce the amount of cement required and provide some improvement on the properties of both fresh concrete mixture and hardened concrete[74] [136]. Usually, limestone powder is categorized as a kind of inert filler because limestone powder itself

does not have pozzolanic activity, but with the decreasing particle size of the limestone powder, especially when it is smaller than the cement grains or co-added with SCMs like fly ash, the limestone powder will possibly participate in the hydration process and affects the properties of the concrete[78]. In this part, the effect of micro-calcium carbonate on the hydration process, workability and mechanical properties are reviewed.

For the hydration process, as discussed above, the micro calcium carbonate would have both chemical and physical effects (including filler effect, dilution effect and nucleation effect) on the cementitious materials, results in the differences in the cumulative hydration heat, hydration heat flow and the hydration product. Those effects can be influenced by the particle size, content and crystal structure of micro calcium carbonate.

When added into cement, micro limestone powder majorly acts as fillers and nucleus to create the filler effect and the nucleation effect. In this case, the smaller particle size means higher specific surface area and higher surface energy, so smaller limestone powder particles would be able to fill more pores than larger particles to improve the pore structure, and the higher specific surface area also provides more nucleus for the hydration products (calcium silicate hydration, C-S-H) to grow. When the nucleation is accelerated, the local concentration of the cementitious material e.g., C_3S is lowered, resulting in an acceleration of the solution of C_3S, causing dilution effect, further accelerating the hydration process. Overall, the smaller the particle size, the better the physical effects, and the faster acceleration effects on the hydration process. However, when it comes to the limestone powder smaller than cement grains, the effects

on the hydration process are quite different, leading to the chemical effect, resulting in the formation of carboalumnates [74, 136-138].

The content of limestone powder also affects the main mechanism of hydration of cement. In general, more limestone powder would provide more nucleation sites for the formation of C-S-H, improving the nucleation effect, which further accelerates the hydration process [139].

As for the crystal structure, calcite has been proved to have both physical and chemical effects on cementitious composites, while aragonite does not have such effects [140].

The workability of fresh mixtures incorporating limestone powder is influenced by the particle size, content and surface morphology. Viscosity increases as the particle size of the limestone powder decreases, especially when the limestone powder has the same particle size as the cement grains, due to the filler effect and high specific area.

The workability of fresh mixtures containing limestone powder mainly depends on its particles. Size, content and surface morphology. Due to the higher specific surface area, the finer limestone powder would require more water to achieve normal consistency [141]. Therefore, self-consolidating concrete prepared with finer limestone powder may have better segregation resistance and better flowability [138]. The substitution ration also increases both the viscosity and yield stress for higher specific surface area. Crystal structures and the purity of the micro calcium carbonate would also affect the workability [142].

The mechanical properties of cement-based composites containing limestone powder depend on particle size, content and form. The early-age compressive strength is

increasing with finer calcium carbonate particles, due to the acceleration effects on the hydration process [143]. But because of the eminent dilution effect that finer limestone particles have, the long-term strength is decreased[136, 139, 144]. With increased substitution content, the compressive strength and the flexural strength is decreased, because of the lack of cementitious reactivity of limestone powders and the dilution effect.

2.1.5.2. Nano-calcium carbonate. Nanoparticles are commonly defined as materials with a particle size of less than 100 nm [145] and can make revolutionary changes in bulk material properties[64]. The addition of nano particles in cementitious composites can significantly improve their mechanical properties and durability [146]. Among these nanoparticles, nano-calcium carbonate is one of the most widely used nanoparticles in the construction materials [147]. In this review, the restriction on the particle size of nano particles is broadened from 100nm to 1μm. Compared with micro calcium carbonate, nano calcium carbonate particles has a more important impact on the hydration process, processability, mechanical properties and durability of hydraulic composites[148], for the differences in the particle size.

First of all the hydration process, the effect of nano-calcium carbonate on the hydration process of cement depends on its content, particle size and crystal structure. Nano-calcium carbonate has a significant acceleration effect on the hydration process due to the nucleation effect. Also, when the C_3S is dissolved in water, the calcium ions would be absorbed onto the surface of the nano-calcium carbonate because of the high surface energy, resulting in a local drop on the concentration of calcium ions, which accelerates the dissolution of C_3S. Both dilution effect and nucleation effect of nano-calcium

carbonate caused an acceleration of the induction period[149, 150] and the overall hydration process. Moreover, evidence show that nano-calcium carbonate can also react with C3S to form C-S-H gel and $Ca(OH)_2$ and this may be also the reason for earlier and higher hydration heat[151]. Same as it of the micro calcium carbonate, the nano-calcite has better acceleration effect than the nano-aragonite [152].

For the workability, generally speaking, the workability of nano calcium carbonate incorporated cementitious composites have the same trends as it of the composites incorporated with micro calcium carbonate[78]. Since the particle size of the nano particles are small enough, the intensity of the dilution effect and filler effect may differ with the change of the particle size and replacement content[153]. But the overall trends for the single factors are the same[154].

And for the workability, the mechanical properties of nano-calcium carbonate incorporated cementitious composites mainly depend on its content. The overall trend is the same as the micro calcium carbonates: With the increasing dosage of the nano calcium carbonate, the long-term compressive strength would first increase then decrease, while the early-age compressive strength keeps increasing due to the acceleration effect. There are reasons for the trend: The addition of nano-calcium carbonate can have acceleration effects on the hydration of cement due to the physical effects and the chemical effect, and the effect is strengthened with the increase of the nano-calcium carbonate content. However, when the dosage is large enough, due to the lack of cementitious reactivity, the nano-calcium carbonate itself will not provide sufficient strength for the structure, just like the micro calcium carbonate particles. As commonly seen in nano particles, the agglomeration would form clusters of nano particles that can

seriously reduce the development of the compressive strength. Plus, unlike the micro calcium carbonates, the filler effect of the nano calcium carbonate will form denser matrix that would limit the development of the hydration products, which further halters the development of the compressive strength [155] [151].Evidence show that incorporating nano calcium carbonate with conventional SCMs would help the later-stage strength development[156] and the development of interfacial transition zone[157]. So, adding nano calcium carbonate along with conventional SCMs may be beneficial for both short-term and long-term strength.

2.1.6. Summary. Both micro and nano calcium carbonate have the physical and chemical effects that would affect the properties of the cementitious materials. Generally speaking, the effects can be concluded as a typical early strength agent that accelerates the hydration process of the cementitious material, and when the particle size is small enough, an addition chemical effect will occur, forming carboaluminates. So, incorporating micro and nano particles will both benefit the early-stage strength development, and the nano calcium carbonates have better effects due to the higher surface area. The overall effects are influenced by multiple factors e.g., particle size, content, and crystal structure of the calcium carbonates. It is important to note that due to the lack of cementitious activity, the incorporation of calcium carbonate particles—no matter micro or nano—would not provide strength for the structures by themselves, meaning that with the increasing calcium carbonate content, the strength development may be limited, but with the incorporation of SCM, the long-term strength problems seem to be overcome. Though nano calcium carbonates have more eminent beneficial effects than the micro calcium carbonate, the agglomeration problem is still a crucial

factor that would impact the strength development of the cementitious materials. That is to say, if the agglomeration problem can be solved, the major problem in strength development at higher nano calcium carbonate can be mitigated.

2.2. MSWI ASH AND ITS APPLICATIONS AS CEMENTITIOUS MATERIALS

Municipal solid waste incineration (MSWI) ash is the major byproduct from the waste incineration plants, usually disposed by landfilling. However, with the increasing production of MSWI ash and the shortages of landfills, the better solution for disposing the MSWI ash is getting more attention. Among the proposed methods, some researchers looked into the cementitious materials.

2.2.1. General Background. 292.4 Mt of municipal solid waste (MSW) is produced in the US every year, more than 50% of it was landfilled, 32.1% is recycled or composed, and 11.8% is used in waste-to-energy (WtE) plants[158]. Since landfilling is occupying enormous amount of space and the leaking could cause long term secondary pollution, WtE plants, as an efficient way to decompose unrecyclable MSW and to generate electricity, is getting more attention by the researchers. The WtE process can reduce MSW mass by 70% and volume by 90%[159]. However, using/upcycling the residue, namely, MSWI bottom ash and fly ash, remains a great challenge[160].

The technical problems of MSWI bottom ash and fly ash – which hinder their upcycling – are their high variability in chemical composition and high contents of undesired substances, such as chloride, alkalis, heavy metals (HMs), and unburned carbon[159, 161, 162]. While the latter issue can be addressed to some extent, the high chemical variability is a significant roadblock hindering the ashes' upcycling, since it is

difficult (if possible) to manufacture consistent products from highly variable raw materials. If these problems can be addressed, the ashes will become an asset from which critical elements can be mined[163], regular metals can be recovered[164, 165], and the rest can potentially be turned into construction and/or functional materials[162, 165]. It is estimated from the data cited above[158, 159, 166] that, if all currently landfilled MSW is fed into WtE streams, the amount of this waste (asset) will surge to 50~80 Mt/year only in the US, which is sufficient to meet the requirement of SCMs in the construction market.

2.2.2. State of the Art Research. Current resource-recovery practices from MSWI ashes have focused on regular and critical metals. However, majority of the ashes comprises nonmetallic compounds, represented by CaO, SiO_2, Al_2O_3, and Fe_2O_3. As a result, the ashes' chemical makeup are analogous to those of cements, supplementary cementitious materials (**SCMs**), or regular glass/ceramics. Therefore, MSWI ashes have been widely recycled in portland cement (PC)[167], sulfoaluminate cement (SAC)[168], Eco cement[169], concrete (as aggregate and SCMs[170], ceramic tile/paver[171], and adsorbent/zeolitic products. Owing to contamination of the ashes by toxic substances and detrimental ingredients, the ashes have to be treated before they are recycled. Typical treatment methods include separation (e.g., washing, leaching, and electrochemical process), immobilization; and thermal treatment (e.g., vitrification and fusion)[159, 172, 173]. Even after treatment, the ash-uptake rates in different applications are low. For example, the uptake of bottom ash in cement clinker production, SCMs, and concrete aggregate are less than 50%, 15%, and 50%, respectively; and that of fly ash in cement clinker production is substantially lower (i.e., 0.33%-10%[174, 175]). Apart from

detrimental ingredients that limit the uptake rates of ashes in products (e.g., chloride ions in cement), the extreme chemical variation of the ashes is a dominant factor for the aforesaid limitations. According to the literature, the compositions of both fly ash and bottom ash are highly variable. The variations can be represented by the coefficients of variations (COVs) of SiO_2 and Al_2O_3 contents of fly ash and bottom ash – (52%, 64%) and (33%, 43%), respectively. As a benchmark: COVs of SiO_2 and Al_2O_3 of Class F fly ash – the most widely adopted SCMs in construction – are (10%, 11%)[176].

Compared to efforts for reducing undesired substances, studies dedicated to addressing chemical variations of MSWI ashes are scarce. Theoretically, there are two strategies to address this problem: (I) develop products of which the performances are insensitive to chemical variation of ashes; and (II) reduce chemical variation. There are two potential pathways to make products "insensitive" to the ashes' variation (strategy I): (1) introduce an extra thermodynamic force (in addition to chemical reaction) to minimize the effect of ash variation on properties of product; and (2) produce functional materials in which the property variation does not affect usability. An example of the first pathway is to melt MSWI ashes (e.g., in an electric arc furnace[171]), and then cool them to produce glass/ceramics-based products (e.g., architectural tiles). An example of the second pathway is to produce geopolymer/zeolite-based filtration devices for removal of HMs and other contaminants from waste water[177]. Pathways in strategy I have a common limitation: the relevant market size is too small to leverage the enormous amount of ash feedstock (>50 Mt/year). Large markets, for example, cementitious materials (>100 Mt/year), mandate the raw materials to be of stable composition to meet industrial standards; thus, necessitating strategy II.

Strategy II is apparently harder to achieve. The chemical variation of ashes is engendered by extreme variation of the parent waste that is incinerated (i.e., MSW), which is determined by geographical location, residents' daily living habits, incineration conditions, and even season[159, 162]. One may believe that pre-WtE sorting of MSW can reduce its variation in sorted fractions; however, this sorting has been proven to be socioeconomically infeasible (known as "wishcycling"[178]). To date, there is no technology that can reliably and effectively reduce chemical variations of MSWI ashes, though such methods are of great significance to the industry.

2.2.3. Implications. Novel technologies are in urgent need to upcycle MSWI ashes, addressing the compositional variations and upcycle them into value-added products. A special interest is to upcycle the ashes into SCMs to meet the material shortage and decarbonization demand of the cement/concrete industry. For this, the technologies should be able to mitigate the detrimental effects of the ashes and maximize their potential as SCMs, and perfectly, leverage carbon-negative pathways.

3. SYNTHESIS OF NANO-CALCITE WITH BUBBLING METHOD AND THE EFFECTS OF NANO-CALCITE ON THE HYDRATION OF CEMENTITIOUS MATERIAL

3.1. RESEARCH BACKGROUND

Concrete, as the most common construction material, for the relatively low price, good durability, and good accessibility, has been widely used in a variety of buildings and structures since first invented about 200 years ago. As the necessary raw material of concrete production, the cement manufacturing industry is also consuming the most (in all raw materials of concrete) energy and emitting the most carbon dioxide to the atmosphere. Approximately 0.87 tons of carbon dioxide will be generated with the production of each ton of Portland cement, considering the production of Portland cement has already reached to 4.2 billion ton in 2017 and still increasing, according to the U.S. Geological Survey, and the carbon emission has become one of the major problems in this industry. In 2021, the mean concentration of carbon dioxide in atmosphere has reached to 420 ppm [179], and the trend is still rising; some researches also suggested that the concentration will break 550 ppm before 2050. The results of the greenhouse effect are not only the rise of global sea level but also more frequent extreme weathers and an estimation of 18-37% extinction of current species by 2050. So, as discussed in Section 1, breakthrough technologies are needed to reduce the CO_2 embodiment and improve the eco-efficiency of cement and concrete. Use ground or in situ formed calcium carbonate as functional fillers or SCMs can potentially be an effective manner.

Calcium carbonate can be in various polymorphs such as calcite, aragonite, vaterite and amorphous calcium carbonate (i.e., ACC). Among these, calcite is the most

common and stable. Most natural limestone is in the form of calcite. It has been confirmed that incorporation of calcium carbonate will not be detrimental to mechanical properties and even has a positive synergic effect on early-age strength, the hydration process, durability and microstructure of cementitious composites. Hence, much research has been conducted to clarify the effect mechanism of calcium carbonate on cement paste, mortar or concrete. In 1938, Bessey et al. [53] first found the formation of calcium-carboaluminate in the hydration process of cement when calcium carbonate was incorporated, which was called the chemical effect of calcium carbonate, and similar results have been found in later studies. Subsequently, a large number of studies were conducted on the role of calcium carbonate in cement paste, mortar or concrete. Now it is widely accepted that the density of the matrix can be increased when calcium carbonate is incorporated, because of its filler effect, and the hydration process can be accelerated because of its nucleation effect. When the particle size of calcium carbonate is comparable to cement grains, the dilution effect will be effective to influence the workability and hydration process of cement. However, these effects are not independent and often have a coupling effect on mechanical properties, the hydration process, workability, and durability of cementitious composites because of its particle size, content, and morphology. Recently, the potential of nanotechnology in improving the performance of building materials has been explored. The incorporation of some nano materials has been proved to have positive effects on the acceleration of cement hydration, the increase of early-stage mechanical property and the improvement of the concrete durability.

This section majorly focuses on the influences of nanometer sized calcite manufactured with CO_2 bubbling method on the hydration of the Portland cement paste. The goal is to develop a method that could be used to improve the performance of Portland cement altogether with the use of CO_2 (e.g., that captured from industrial flue gases or direct flue gasses), providing a promising solution for the CO_2 emission control in the cement and concrete industry.

3.2. MATERIALS AND EXPERIMENTS

Nano-sized calcium carbonate particles are to be synthesized, and the product will be added into cement pastes to compare the effects.

3.2.1. Materials and Reagents. Analytical grade calcium oxide (CaO) powder was purchased from HiMedia, India. Food grade carbon dioxide (CO_2) was purchased from Air Gas company. The superplasticizer was purchased from BASF, in a suspension system. The solid content of the superplasticizer tested is ~25%. Commercial Type I Portland cement (Royal White Cement, USA) 42.5 R was used as the binder material for preparing the cement paste. The chemical composition of the cement is shown in Table 3.1. Deionized (DI) water was used as mixing water for preparation of the cement paste. Calcium carbonate nanoparticles were synthesized in a beaker using the preparing protocols mentioned in the next section.

3.2.2. Preparation of Calcium Carbonate Nanoparticles and Suspension. The CaO was mixed in DI water to produce calcium hydroxide ($Ca(OH)_2$) suspensions at the concentrations of 2%, 4% and 8% (w% of the $Ca(OH)_2$ in the final suspension systems or slurries). All the highly diluted $Ca(OH)_2$ slurries are mixed under room temperature (~20

℃), the slurries are all sonicated with SonicQ sonicator under 18W for 10 mins. Then CO_2 is aerated into the suspension at various rates while the suspension is agitated. pH of the suspension is monitored following time while more and more nanoparticles are formed and precipitated. The precipitates are separated and characterized (e.g., via XRD and SEM). When being used an SCM in cement pastes, no separation is needed – the slurry is used as mixing water directly. Additional water was added to each produced slurries to maintain a fixed water content when mixing.

Table 3.1 Chemical composition of cement

Oxide	**Cement(wt%)**	**Oxide**	**Cement(wt%)**
CaO	65.8793	**TiO2**	0.19075
SiO2	18.715	**Mn2O3**	0.086
Al2O3	4.03825	**Cl**	0.07175
Fe2O3	3.5485	**SrO**	0.0525
SO3	2.41	**P2O5**	0.032
MgO	1.73975	**ZnO**	0.0293
Na2O	0.97	**Cr2O3**	0.0107
K2O	0.6555	**LOI**	1.4
		Sum	99.8293

3.2.3. Paste Sample Preparation and Mix Design. The mix designs of the paste samples are shown in Table 3.2. The percentage of CC is based on the mass of CH in

water/suspension. The samples are well mixed, and all the mixing water are sonicated with the SonicQ Sonicator before poured into the cement. The water/binder ratio was set as 0.4 and 0.5, respectively. The mixing water was set to 100g, cross all the sample groups, the nano calcite particles was set as the substitution of the cement. The mixed samples were cast into silicone molds with the dimensions of 2cm×2cm×2cm and then move to the standard moisture curing room with 20℃ and RH>90% for 24h before demolding. After the cubes were demolded, they were subjected to the hydraulic machine for testing compressive strength, after each test, the most representative samples from each strength test were put into small bottles with isopropyl for stopping the hydration. After 24hrs, the samples were then removed from the bottles and put into the oven under 80℃ for 12h for drying, and the dried samples were grinded with disc mill for the purpose of characterizations. The strength tests and sampling were repeated at further ages of 3 days, 7 days, 28 days, and 56 days.

3.2.4. Characterization Methods on Nano-calcite and Paste Samples. All the slurries were sonicated for 10 mins under 18W before subjected to the CO_2 bubbling system. The gas flow rate during synthesis was controlled by the mass flow controller (MFC, Sierra Instrument Smart Trak 200, for CO_2 specially, 0-200 sccm). The pH curves are obtained with a pH meter (Hanna Instrument HI 5222). The pH meter contains three probes: a pH probe, a temperature probe, and an ISE probe; in this experiment, only the data from the pH probe and the temperature probe were analyzed.

After the slurries were fully carbonated, the prepared samples are sonicated for 10 mins under 18W before the test. The particle size distribution curves were obtained with the zeta-sizer, the major detecting range of the zeta sizer is 1-1000 nm. The baseline of

the DI water was also obtained for the reference. Each testing sequence contained 3 major sections, for each section, 100 curves were obtained, and the final particle size distribution curve was the average curve of the total 3 major sections.

Table 3.2 Mixture proportions of cement pastes incorporating CC nanoparticles

No.	CC (%)	SP (g)	OPC (g)	No.	CC (%)	SP (g)	OPC (g)
0.4wc	0	0	200	**0.5wc**	0	0	250
0.4wc+ 2%CC	2	0	200	**0.5wc+ 2%CC**	2	0	250
0.4wc+ 4%CC	4	0	200	**0.5wc+ 4%CC**	4	0	250
0.4wc+ 8%CC	8	0	200	**0.5wc+ 8%CC**	8	0	250
0.4wcSP	0	0.24	200	**0.5wcSP**	0	0.24	250
0.4wc+ 2%CC	2	0.24	200	**0.5wcSP+2%CC**	2	0.24	250
0.4wc+ 4%CC	4	0.24	200	**0.5wcSP+4%CC**	4	0.24	250
0.4wc+ 8%CC	8	0.24	200	**0.5wcSP+8%cc**	8	0.24	250

After the particles were all prepared and well-mixed, take 1mL of the suspension, add 19mL of de-ionized water for diluting. The diluted suspension was then sonicated with the sonicator for 10 mins to break the possible agglomerations between the particles. Then the diluted suspension was put on a silicone wafer, spread, and put into the oven under 60°C for drying. The prepared silicon wafers were then put into the SEM (Raith-

eLine system) for observing and capturing the SEIs (Scanning Electronic Images) with 10kV acceleration voltage to check the morphology of the nano-calcite particles.

The casted paste samples are tested with Tinus Olsen compressive strength tester. The paste cubes at various ages were first pre-loaded under 75lbs for 10s then loaded with the rate of 50lbs per second until failure. The most representative sample in each set was then collected in a small bottle and filled with isopropyl alcohol for stopping hydration. After 24h, the soaked samples were then put into the over under 105℃ for drying (then used as samples for microscopic characterizations).

Powder X-ray diffraction patterns were obtained for all the nano-calcite and paste samples. The suspensions with synthesized calcite were filtered, the solids left were collected and put into the oven under 60℃ for 24hrs. The representative paste samples collected from each test were soaked in isopropyl alcohol for stopping hydration, after 24hrs the samples were collected and put into the over under 80℃ for 12h for drying. The oven-dried calcite samples and paste samples were grinded with disc mill. All the milled samples were analyzed on a Panalytical X'Pert MultiPurpose Diffractiometer with 45kV tension and 40mA current with Cu radiation covering the 2θ range between 10° and 70°.

3.3. RESULTS AND ANALYSIS

The testing results are listed and discussed in this section.

3.3.1. pH Evolution Curves. The pH evolution curves of the calcium hydroxide slurries are presented in Figure 3.1.

For all the groups, a steady stage at the beginning of each group is observed. This is when the CH slurries are supersaturated (the solubility for CH at room temperature is ~0.15%), and excessive CH solids keep dissolving when the dissolved CH has reacted with CO_2, which makes the pH nearly constant at this stage. After the excessive solids are consumed, the pH starts to drop rapidly, and finally neutralized. As expected, the higher the CH concentration, the longer the time needed to break the supersaturation and reach neutrality, because of the larger repository excessive CH given constant CO_2 flow rate.

With the same CH dosage, the introduction of SP has decreased the initial pH for the saturated CH slurries. The groups without SP start at around pH = 12.5; while after

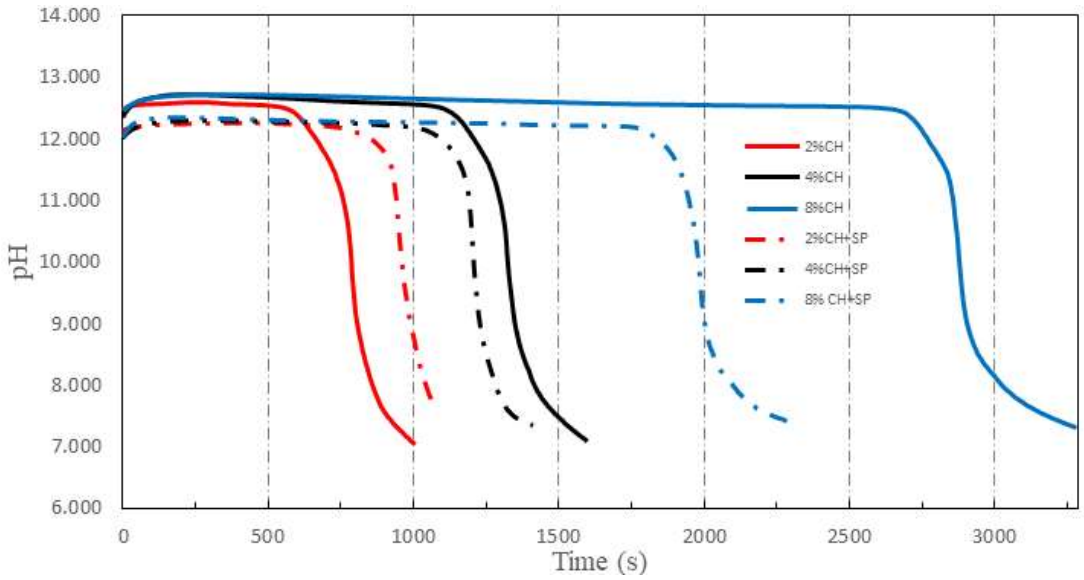

Figure 3.1 pH evolution of Ca(OH)2 suspensions following CO2 aeration

adding the SP, the initial pH has been lowered to around 12, indicating a possible decrease in the solubility of CH. An increase of reaction rate has been observed for the

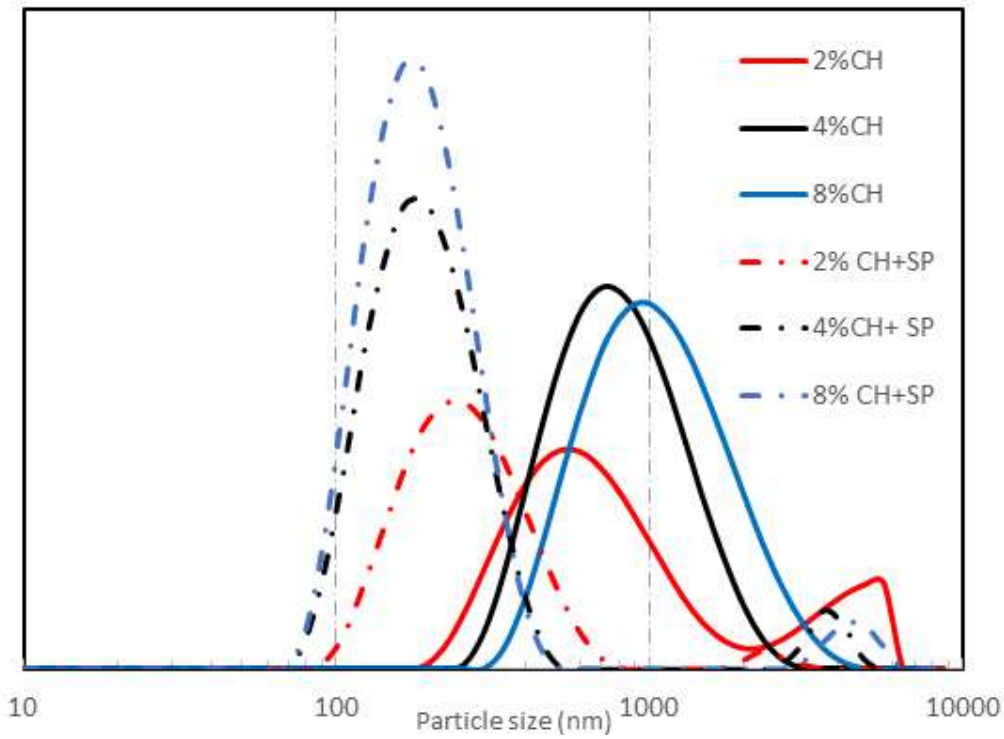

Figure 3.2 Particle size distribution curve of synthesized calcite by zeta sizer

samples with SP, except for the 2%CH sample. The acceleration effect of reaction rate is more obvious in the group with higher CH dosage. But for the 2%CH group, the introduction of SP slowed the reaction rate.

3.3.2. Particle Size Distribution. Figure 3.2 shows the particle distribution curves of nano calcite formed under various conditions, as determined by zeta sizer. Note that the range of the Zeta sizer is below 10μm, so the particles larger than 10μm (if any, e.g., strongly agglomerated particles) are not counted.

According to the curves, it is obvious that the addition of superplasticizer provides a positive effect on controlling the particle size of the synthesized calcite particles. The major peaks of all the samples with superplasticizer are located around 200nm, while the groups without superplasticizer have their major peaks located around

600-800nm (likely due to agglomeration, as will be shown by SEM images in the next section). For the groups with superplasticizer, the particle size decreases with the increasing CH concentration, this trend agrees with the results from [131]. But for the groups without superplasticizer, the trend is different: higher initial CH concentration resulted in larger particles (due to agglomeration). Moreover, the groups with superplasticizer show a small hump at larger particle size, compared with the SEM images and the literature [117]. It is speculated that the small humps are caused by the agglomeration of the synthesized particles or the leftover CH. For the groups without superplasticizer, the small humps are not shown, apart from 2%CH sample that shows a trend of another hump larger than 10μm, compared with the SEM images. It is reasonable to speculate that larger agglomerations are also included in 4%CH and 8%CH samples without superplasticizer that could not be detected using the Zetasizer.

3.3.3. Scanning Electron Microscopy Images. Figure 3.3 shows the scanning electron microscopy images of the in situ formed calcite nanoparticles.

It can be observed that all the samples contain nano-size particles. For the groups that do not have the superplasticizer, the particles tend to form clusters, the edges of the particles are not easily distinguished. The particles from the groups with superplasticizer are well-dispersed, the particles are not forming agglomerations, and the edges of the particles are clearer than the groups without superplasticizer. The particles in all six samples have the similar shape that close to a spindle, but with the increase of the concentration of calcium hydroxide slurries, the particles tend to grow the in axile direction (i.e., larger aspect ratio). The calcite particles in the samples with lower calcium hydroxide concentration have sharper ends, while the sample with the highest

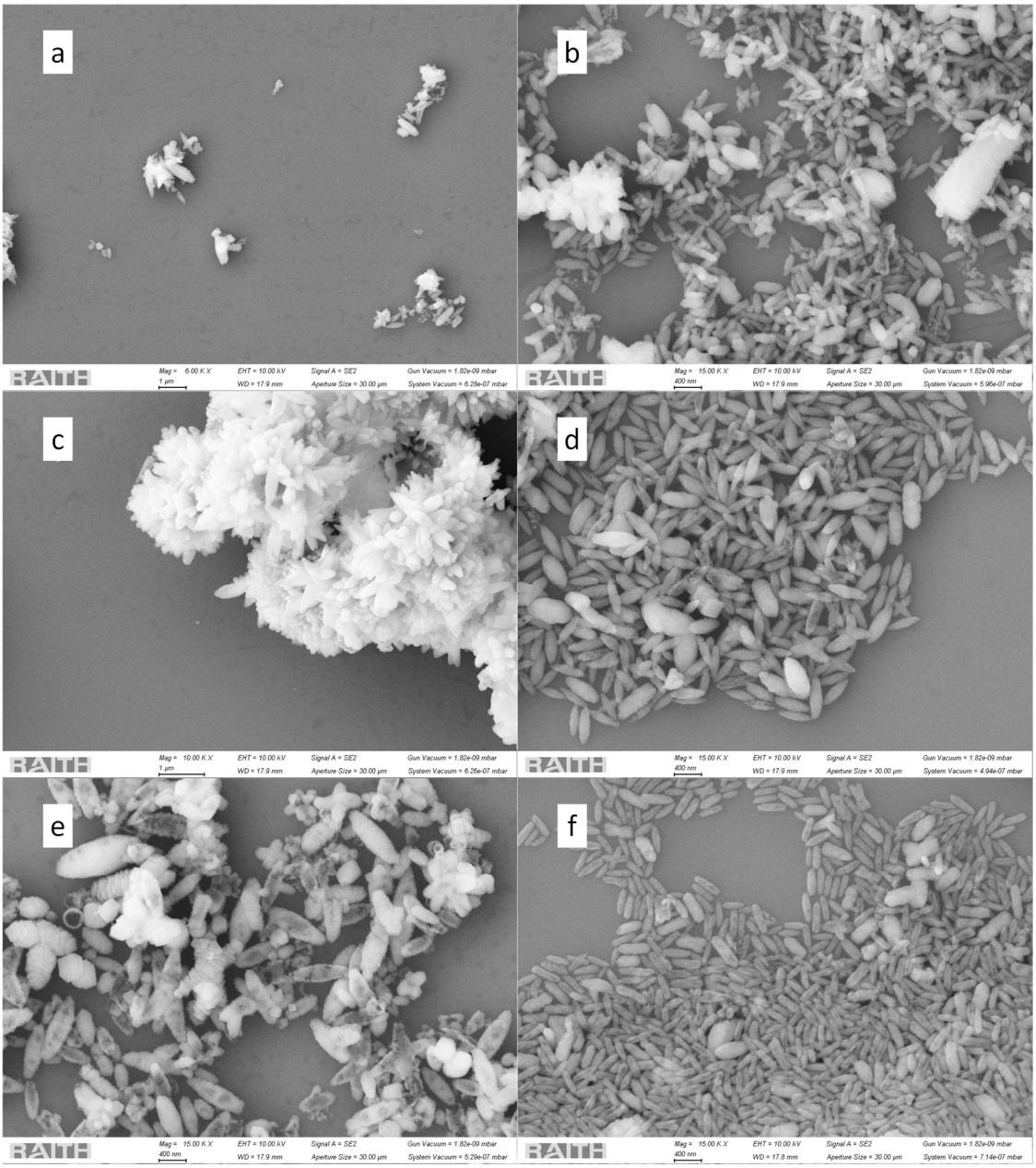

Figure 3.3 The SEIs of synthesized calcite. a) 2%CC, no SP. b) 2%CC, SP. c) 4%CC, no SP. d) 4%CC, SP. e) 8%CC, no SP. f) 8%CC, SP.

concentration are forming a smoother shape that close to rice particles. All the particles have the similar size: the lengths are all ~400nm and the widths are ~80nm, so the

synthesized particles can be classified as fine particles (100-2500nm), but close to nano particles.

3.3.4. XRD Patterns of Synthesized Calcite Particles. The XRD patterns for all the synthesized, oven-dried particles are shown in Figure 3.4.

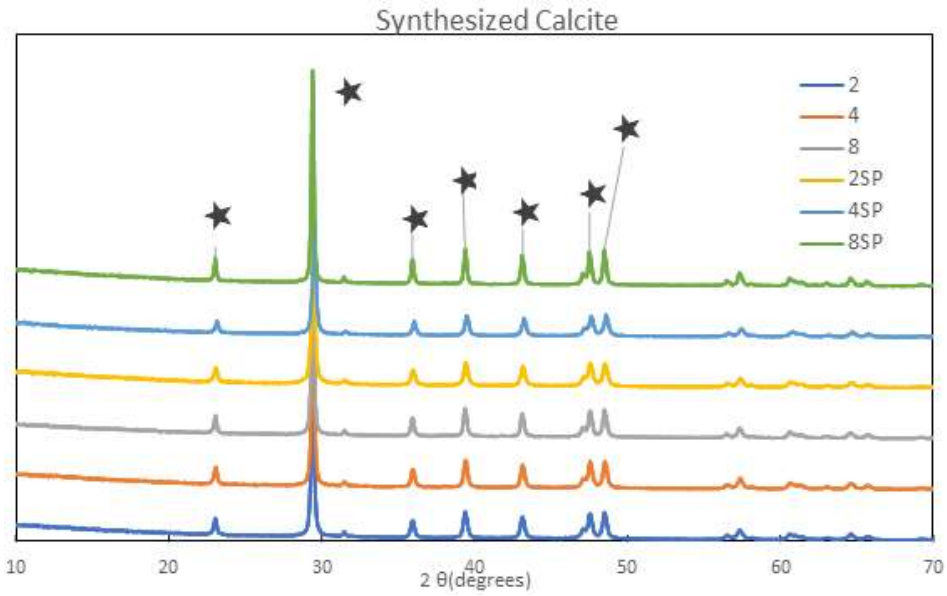

Figure 3.4 XRD patterns of nano calcite synthesized under different conditions

It can be seen that all the major significant peaks from the oven-dried powders match with the powder diffraction file of $CaCO_3$-calcite. There are no obvious minor phases detected, not even residual calcium hydroxide ($Ca(OH)_2$), indicating that the $Ca(OH)_2$ has been completely carbonated; and no calcium bicarbonate was formed neither. Crystallinity does not seem to be affected by $Ca(OH)_2$ concentration and incorporation of superplasticizer. Effect of Nano-calcite on C_3S Hydration. The effects of nano-calcite, synthesized *in situ* in mixing water, on hydration of C_3S were studied using

micro-calorimetry. The results are shown in Figure 3.5. Because of the small dosages, the overall effects of the nano-calcite are not significant.

As show in Figure 3.5(a), within the first day, incorporation of the nano-calcite could accelerate the hydration of C_3S. The higher the dosage, the more significant the influence is. The 8% case showed the most significant effect – the hydration heat peak is advanced by about 2 hours (peak time points: ref – 11.7 h; 2% and 4% - around 10.9 h; 8% - 9.6 h). Figure 3.5(b) is consistent with Figure 3.5(a), showing more cumulative heat in the first 24 h, but this superiority vanishes within the first 3 days.

3.3.5. Compressive Strength of Nano-calcite Modified Cement Paste. The evolution of the compressive strength of the 16 studied paste samples at different stages from 1 to 28 days is presented in Figure 3.6.

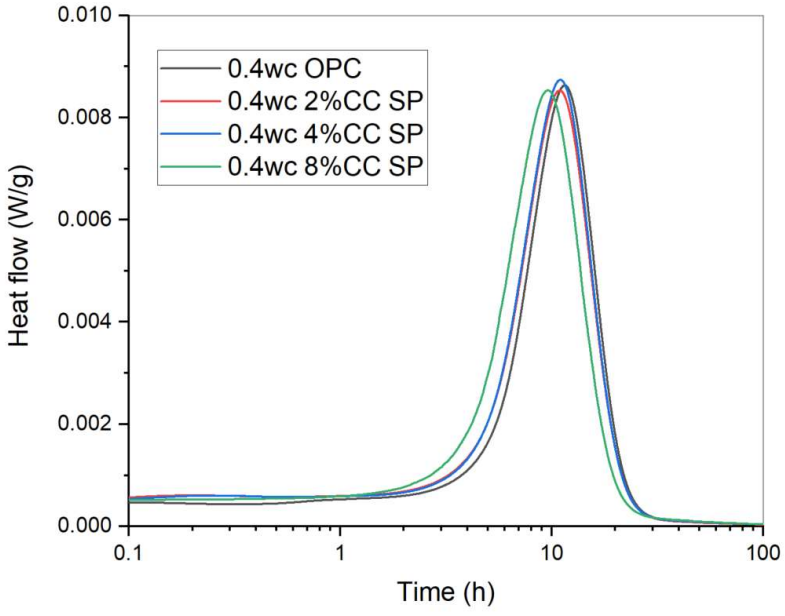

(a)

Figure 3.5 Micro-calorimetry of nano-calcite incorporated C_3S pastes: (a) Heat flow; and (b) Cumulative heat.

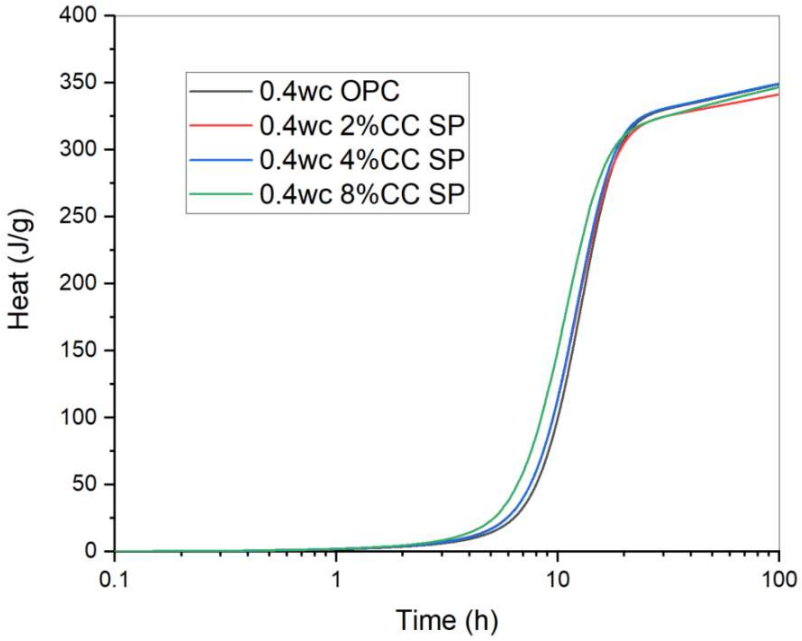

(b)

Figure 3.5 Micro-calorimetry of nano-calcite incorporated C_3S pastes: (a) Heat flow; and (b) Cumulative heat.(Cont.)

It is obvious that the incorporation of nano-calcite does have influences on the compressive strength of paste samples, especially at early stages. For the 0.4 w/c group, an increase of the compressive strength at early stages (1 day to 7 days) were observed, especially for pastes cured for 3 days. The compressive strength is growing along with the increase of the nano-calcite dosage, cross the groups with/out the incorporation of superplasticizer. Superplasticizer added during calcite synthesis appears to have positive effect on compressive strength, due to improved dispersion of the nanoparticles (see Figure 3.3). The superiority of the nano-calcite regarding strength development is maintained until the age of 7 days. However, at a later stage, on the age of 28 days,

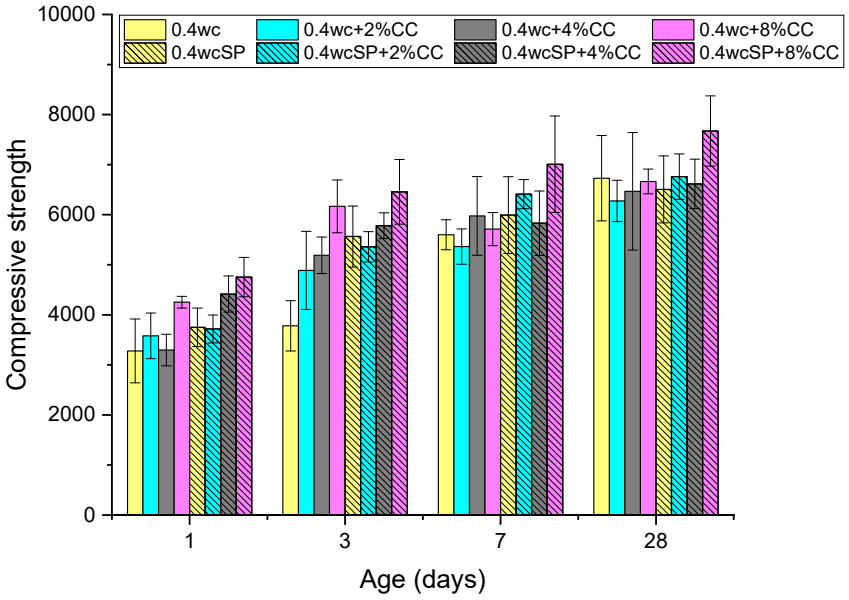

(a)

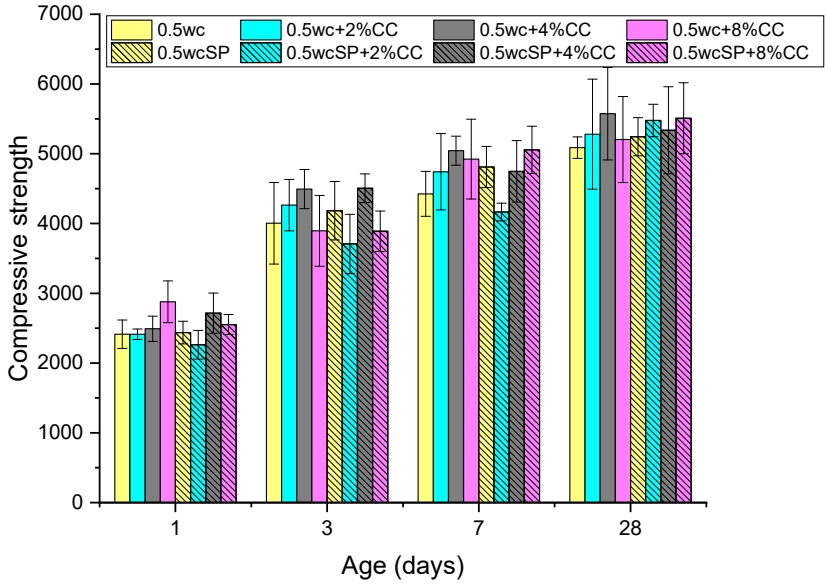

(b)

Figure 3.6 The evolution of compressive strength of paste samples. a) 0.4 w/c pastes. b) 0.5 w/c pastes.

the compressive strength of the nano-calcite incorporated pastes are not higher than the control groups anymore. All these trends (less significant as compared to the w/c=0.4 group) can be found in w/c = 0.5 samples too: at early stages, the samples with the incorporation of nano-calcite have different degrees of increase in compressive strength; while at later stage, the strength growth are lower than the control groups. This observation confirms that the *in situ* nano-calcite only positively affect the early-age strength as an accelerator; which is consistent with the effect of other commonly used accelerators.

3.3.6. Thermal-gravimetric Analysis (TGA). To confirm the effect of the nano-calcite on early-age hydration of cement, thermogravimetric analysis (TGA) was conducted on 1-day aged cement pastes(w/c=0.5) with various dosages of nano-calcite (prepared with/without superplasticizer). The results are collected in Figure 3.7.

As shown in Figure 3.7, the incorporation of nano-calcite tends to increase the amount of C-S-H, CH and other hydration products, with decomposition temperatures not higher than 500℃. However, it is unclear how the amount of total hydrate water is affected, since the amount of calcium carbonate can be determined due to the interruption of the added calcite – calcium carbonate (which can also be formed due to carbonation of calcium hydroxide formed from cement hydration). The peaks between 550℃ and 750℃ are consistent with the dosage of added nano-calcite.

3.3.7. XRD Characterization. XRD results shown in Figure 3.8 further confirms the impact of nano-calcite on early-age hydration of cement. As shown in the figure, at the age of 1 day, the higher the dosage of nano-calcite, the more CH (which serves as an indicator of degree of hydration of cement) can be seen.

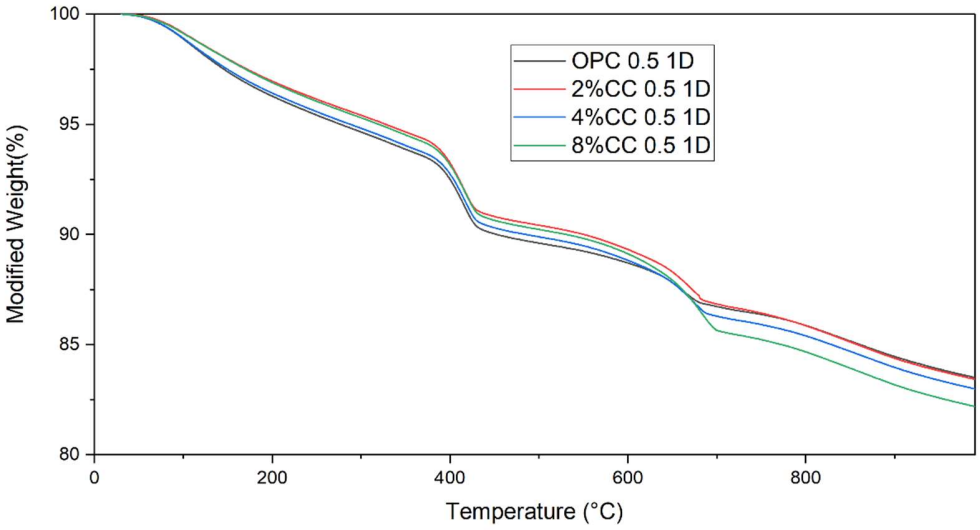

(a)

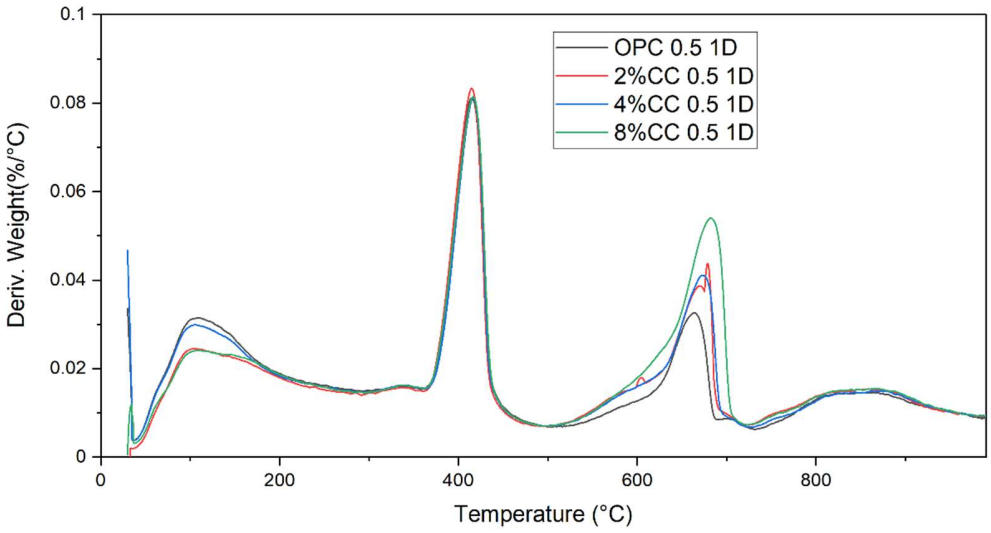

(b)

Figure 3.7 TGA of 1-day aged cement pastes (w/c=0.5) with various dosages of nano-calcite (prepared with/without superplasticizer): (a) TGA, without SP; (b) DTG, without SP; (c) DTG, with SP; and (d) DTG, with SP.

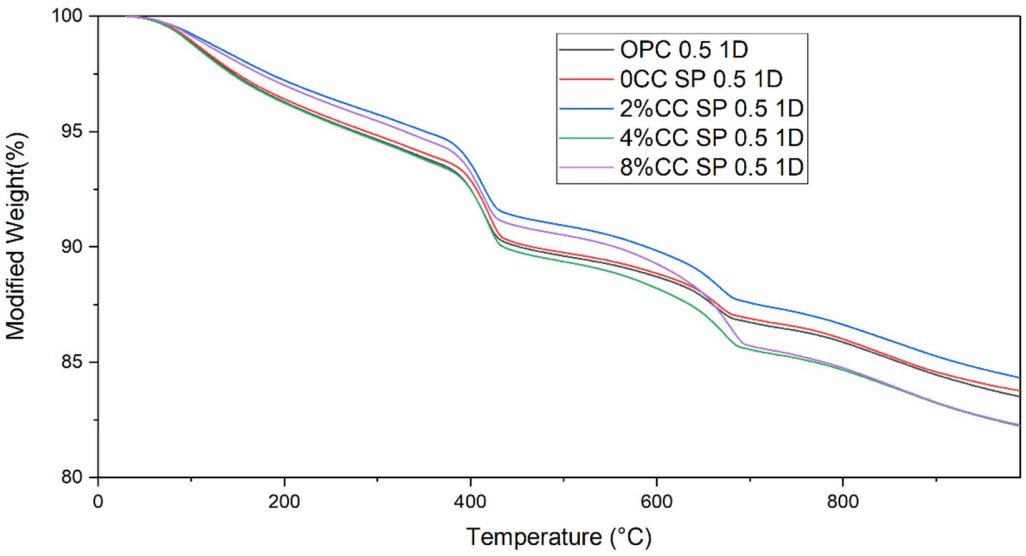

(c)

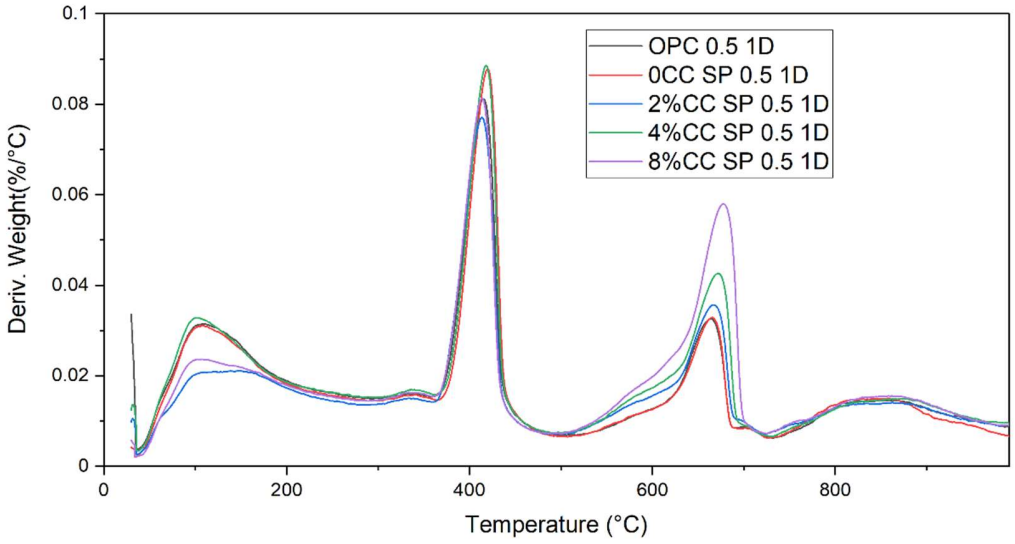

(d)

Figure 3.7 TGA of 1-day aged cement pastes (w/c=0.5) with various dosages of nano-calcite (prepared with/without superplasticizer): (a) TGA, without SP; (b) DTG, without SP; (c) DTG, with SP; and (d) DTG, with SP. (Cont.)

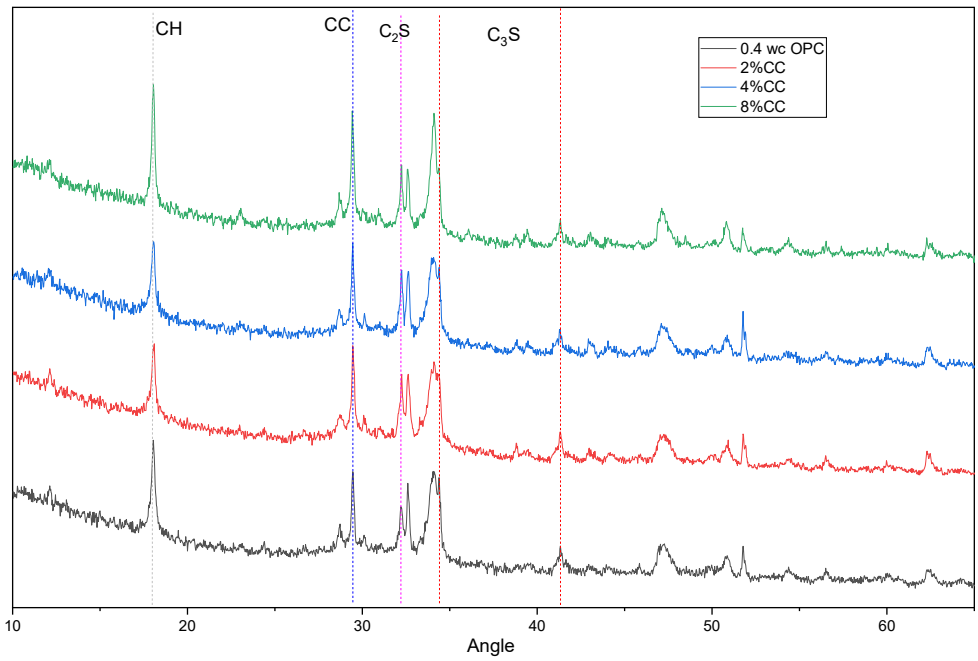

(a)

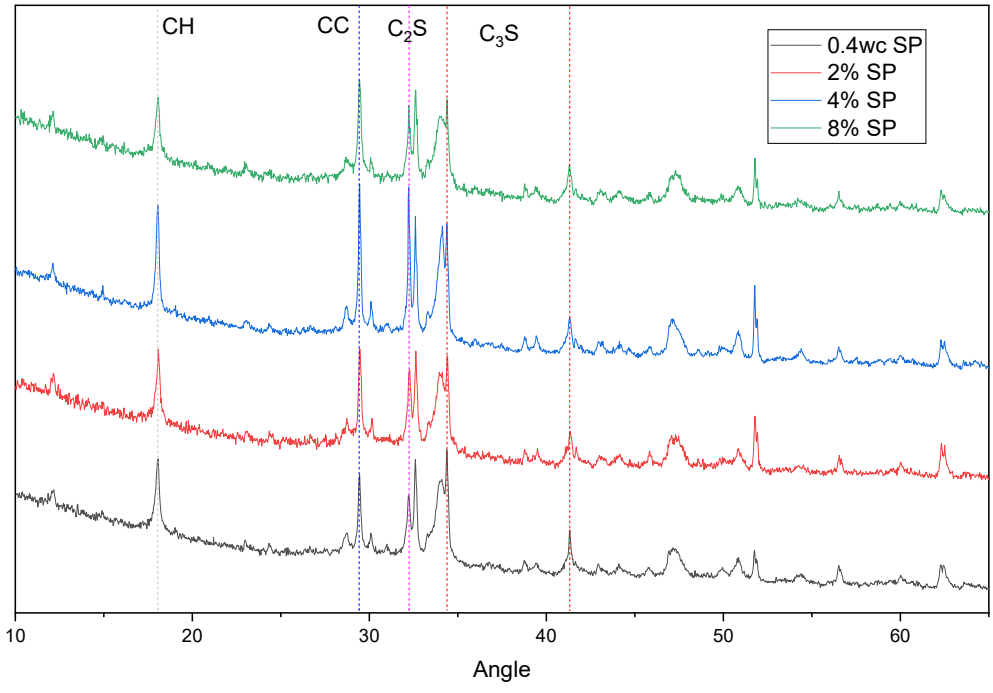

(b)

Figure 3.8 XRD of 1-day aged cement pastes with various dosages of nano-calcite (prepared with/without superplasticizer). a) w/c=0.4, without SP. b) w/c=0.4, with SP. c) w/c=0.5, without SP. d) w/c=0.5, with SP.

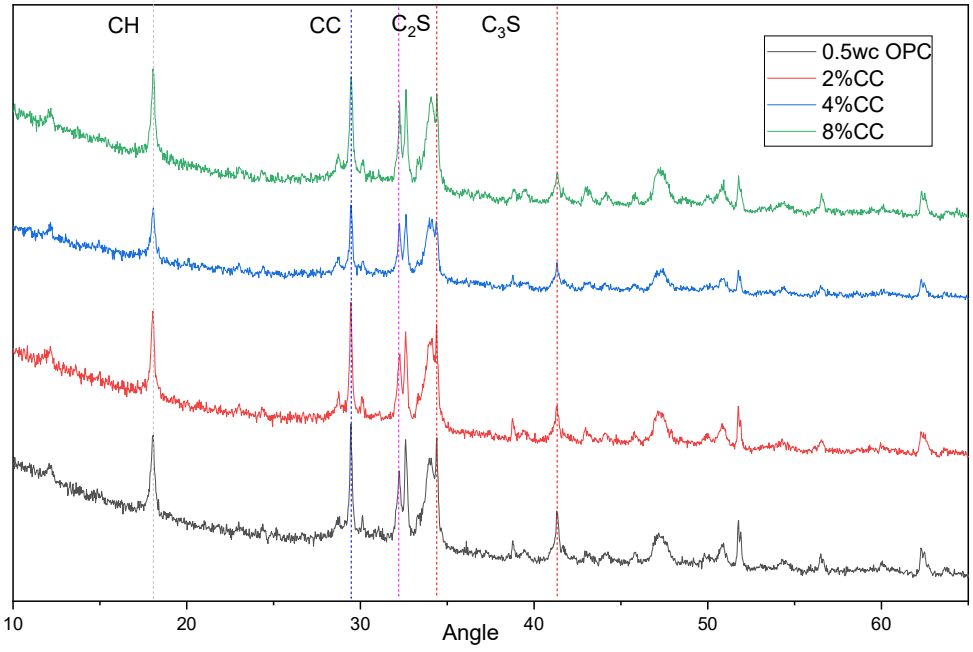

(c)

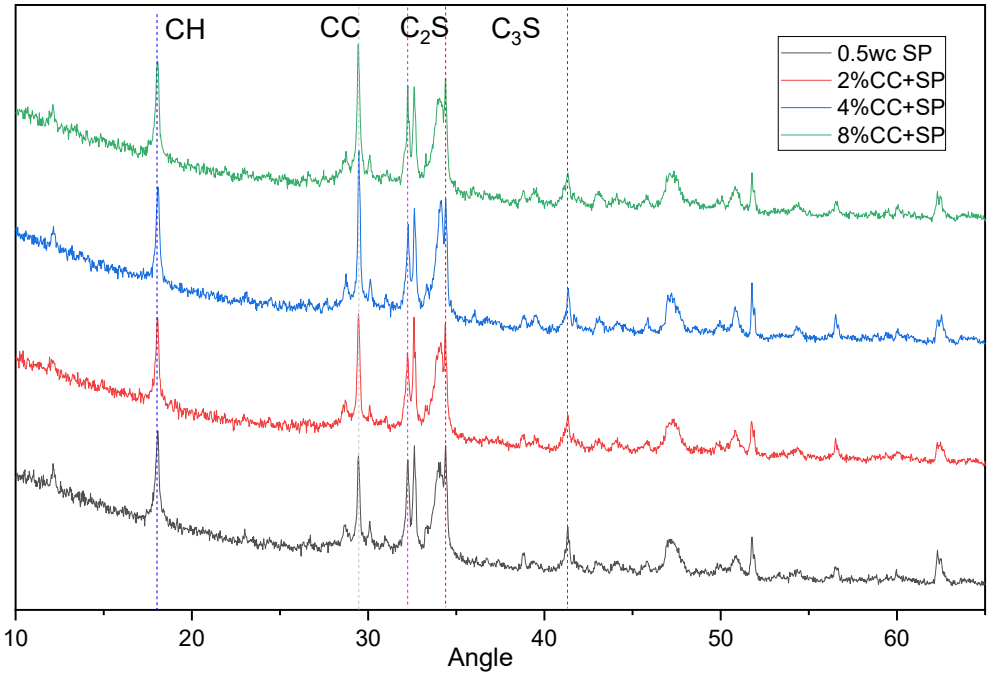

(d)

Figure 3.8 XRD of 1-day aged cement pastes with various dosages of nano-calcite (prepared with/without superplasticizer). a) w/c=0.4, without SP. b) w/c=0.4, with SP. c) w/c=0.5, without SP. d) w/c=0.5, with SP. (Cont.)

3.4. DISCUSSION

This study demonstrates that the synthesis of nano-sized calcite particles can be achieved with CO_2 bubbling method under room temperature, and the morphology is comparable to the data from the literature [87, 114, 121]. The products may have different morphology; but, according to the XRD patterns, the products are all calcite, no other phases were detected, which is consistent with [87]. Such nano-calcite particles are synthesized *in situ* in CaO or CH suspensions, which can be used to prepare C_3S or cement pastes. As shown in this study, the nano-calcite, when added at small dosages, can accelerate hydration reactions (of either clinker or cement) and, thus, improve the early-age strength. However, similar to other normally used accelerators, the nano-calcite does not help with long-term strength. As an important implication, this technology might be an inherent partner for weak pozzolans (e.g., class F fly ash and other alternative pozzolanic SCMs), since the latter group of materials typically retard early hydration reactions but benefit long-term strength development. Since a calcium source is needed to produce such nano-calcite, another implication is that, some industrial solid wastes especially high-calcium wastes (e.g., steel slag and off-specification ashes) might be processed by the developed CO_2-bubbling method to seek possibilities of "upcycling". This concept will be proven preliminarily in Section 4.

3.5. CONCLUSIONS

Through the studies presented in this section, the following conclusions can be drawn:

(1) Through a room-temperature CO_2-bubbling method, calcite nanoparticles can be synthesized *in situ* in diluted $Ca(OH)_2$ (CH) slurries (up to 8% CH by weight of suspension). Agglomerations were formed in all the samples.

(2) The average particle size of the particles is improved by the addition of superplasticizer, the average particle size is lowered from ~800nm to ~200nm, and the agglomerations are mitigated by the addition of superplasticizer.

(3) The nano-calcite suspension can be used as mixing water to prepare cement-based materials; in this case, the hydration reactions (of either clinker mineral or Portland cement) will be accelerated.

(4) As a direct influence, the acceleration effect of the nano-calcite results in improved early-age compressive strength (i.e., up to an age of 7 days); however, such superiority of strength improvement vanishes before an later age of 28 days. So, the nano-calcite acts like a typical accelerator.

4. UPCYCLING MUNICIPAL SOLID WASTE INCINERATION ASHES FOR CONCRETE PRODUCTION USING CARBON DIOXIDE

4.1. RESEARCH BACKGROUND

The US is generating 292.4 Mt of municipal solid (MSW) waste every year, based on the EPA data published in 2019 [180], of which more than 50% is landfilled, 32.1% is recycled or composed, and 11.8% is used in waste-to-energy (WtE) plants [181]. Around 140Mt of MSW has been landfilled since 1990, but this number may be 100Mt less than the actual MSW landfilled each year [182]. Enormous landfill has occupied large amount of space and has caused environmental pollutions, and the leaks could cause long-term secondary environmental pollution problems. Thus, the alternative ways to reuse and redirect the MSW from landfills are gaining more focus [183]. However, because of the socioeconomic and ecological limitations of recycling and composting, WtE and converting the residue into value-added products have been considered as promising strategies to alleviate the landfills. As an efficient way of MSW treatment, incineration can convert waste into heat and electricity, and significantly reduce the waste mass by 70% and volume by 90% [181, 184, 185], but still, the recycle and reuse of municipal solid waste incineration (MSWI) ashes remains a great challenge. There are 75 MSW incineration plants in the U.S, most of them are located in the eastern states [186], the major residue produced from those MSWI plants are MSWI bottom ash (BA) and fly ash (FA). In the U.S., the different MSWI ashes are combined and disposed of in sanitary landfills[187], while in the European countries, the ashes are managed separately [181]. The chemical compositions of the MSWI ashes are complicated, due to the high concentration of potentially toxic elements (PTEs), e.g., Cr, As, Pb, and Zn, and organic

pollutants [188, 189]. That's why the MSWI ashes are categorized as hazardous waste, limiting the potential application of the MSWI ashes. Among the major components, the FA is considered to be more toxic than MSWI BA for the higher concentrations of heavy metals, salts and micropollutants while BA is more steady and often considered as benign material for the low leaching potential [190, 191]. So, the use of BA is more encouraged. In many countries, BA is considered to be a suitable substitute for the aggregates in concrete structures and pavements[192]. However, when adding to the cement-based materials, some deteriorations are observed due to the deteriorating substances such as metallic Al, Cl and highly soluble salts[170, 193, 194]. So, the upcycle is necessary for the better utilization of the MSWI BA. Considering the relatively high calcium content in MSWI BA, using gaseous carbon dioxide as a upcycle method has been studied by many researchers[195].

In this study, we used MSWI ashes provided by York County as replacement of Portland cement to investigate the impacts of the MSWI ashes on the hydration and mechanical properties of cement pastes. By separating BA and upcycle with CO_2, the potential upcycling methods are proposed.

4.2. MATERIALS AND EXPERIMENTS

The materials and details for each experiment are explained in this part.

4.2.1. Materials. An ordinary Portland cement conforming to ASTM C150 Type I was used as the major binder material for the preparation of the cement pastes. The chemical composition of the OPC is the same as in the previous section, as shown in Table 3.1. Three batches of municipal solid waste incineration (MSWI) samples were

received from York County, collected in 11/2020 – 2/2021. Each batch included six types of samples: ferritic dirt (FD), small aggregate (SA), sand (SD), filter cake (FC), (unsorted) bottom ash (BA), and fly ash (FA). It is worth to note that, among the six types of samples, the FD, SA, SD, and FC samples are the four fractions sorted from the unsorted BA. Figure 4.1 displays typical optical microscopic images of the ashes/fractions.

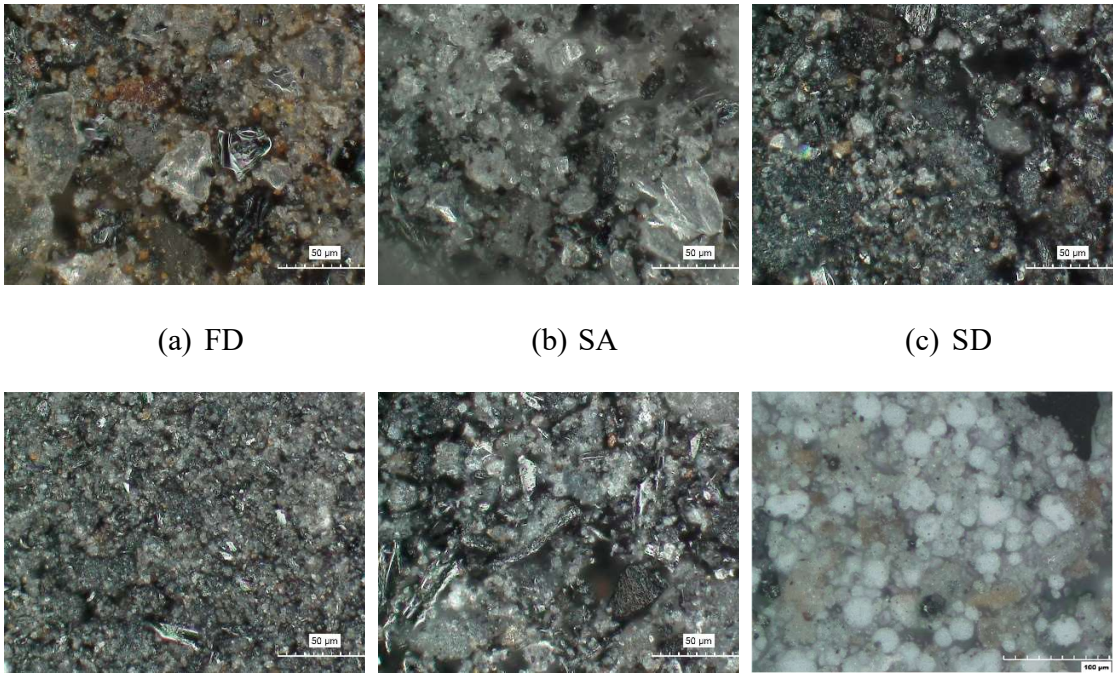

(a) FD (b) SA (c) SD

(d) FC (e) BA (f) FA

Figure 4.1 Typical optical microscopic images of the ashes/fractions.

The brownish ferritic components in FD, glass components in SA and SD, fine powder nature of FC, and spherical particles in FA can all be clearly seen, consistent with their intrinsic characteristics. The MSWI samples were upcycled and used as

Table 4.1 Chemical compositions of the first batch of MSWI sample.

No.	**1**	**2**	**3**	**4**	**5**	**6**
Sample	**Ferritic dirt (FD)**	**Small aggregate (SA)**	**Sand (SD)**	**Filter cake (FC)**	**Bottom ash (BA)**	**Fly ash (FA)**
Na_2O	3.248	4.785	1.265	2.554	1.535	0.938
MgO	2.378	2.072	3.527	3.366	3.142	2.826
Al_2O_3	11.343	6.621	12.61	9.771	9.016	5.715
SiO_2	42.322	63.055	41.562	23.666	40.477	11.814
P_2O_5	1.274	1.213	2.561	2.614	2.799	1.443
SO_3	1.721	1.19	2.272	7.198	4.333	8.019
Cl	0.569	0.379	1.317	2.064	1.751	10.988
K_2O	0.608	0.754	1.38	1.176	1.331	2.046
CaO	12.901	16.305	20.345	37.354	25.351	51.031
TiO_2	0.55	0.364	1.276	1.745	1.314	1.392
Cr_2O_3	0.189	0.079	0.101	0.085	0.113	0.000308
Mn_2O_3	0.26	0.37	0.195	0.206	0.155	0.085
Fe_2O_3	22.21	2.423	10.432	6.866	7.622	1.489
ZnO	0.39	0.356	1.108	1.26	0.956	2.1
SrO	0.00038	0.000344	0.051	0.073	0.106	0.083

Table 4.2 Chemical compositions of the second batch of MSWI sample.

No.	1	2	3	4	5	6
Sample	**Ferritic dirt (FD)**	**Small aggregate (SA)**	**Sand (SD)**	**Filter cake (FC)**	**Bottom ash (BA)**	**Fly ash (FA)**
Na_2O	4.499	4.445	3.289	0.749	1.538	0.365
MgO	2.322	2.698	3.153	3.126	2.905	2.48
Al_2O_3	9.974	8.169	10.648	11.869	9.737	6.091
SiO_2	54.751	59.272	38.156	22.821	42.104	12.327
P_2O_5	1.545	1.251	3.22	2.881	2.82	1.289
SO_3	1.408	1.079	3.16	6.999	4.069	7.152
Cl	0.644	0.525	1.943	1.783	1.898	9.437
K_2O	0.729	0.823	1.381	1.176	1.325	1.472
CaO	14.818	16.035	23.531	38.019	24.038	54.135
TiO_2	0.537	0.445	1.303	1.864	1.212	1.635
Cr_2O_3	0.07	0.000457	0.079	0.07	0.084	0.000286
Mn_2O_3	0.112	0.646	0.18	0.211	0.152	0.088
Fe_2O_3	8.176	4.12	8.966	7.039	7.104	1.667
ZnO	0.347	0.4	0.934	1.317	1.046	1.762
SrO	0.068	0.000462	0.056	0.075	0.059	0.074

Table 4.3 Chemical compositions of the third batch of MSWI sample.

No.	**1**	**2**	**3**	**4**	**5**	**6**
Sample	**Ferritic dirt (FD)**	**Small aggregate (SA)**	**Sand (SD)**	**Filter cake (FC)**	**Bottom ash (BA)**	**Fly ash (FA)**
Na_2O	2.944	4.148	2.674	2.257	0.786	0.153
MgO	2.86	2.95	3.291	3.255	3.205	2.324
Al_2O_3	11.145	7.74	11.603	8.289	10.036	4.607
SiO_2	45.753	58.691	35.922	21.528	35.802	9.926
P_2O_5	1.842	1.379	3.063	2.58	3.024	1.22
SO_3	1.782	1.145	3.522	7.828	4.424	8.368
Cl	0.721	0.46	1.545	1.879	1.856	7.075
K_2O	0.823	0.762	1.263	1.092	1.373	1.687
CaO	15.633	18.593	25.192	41.438	29.575	59.621
TiO_2	0.6	0.354	1.559	1.931	1.384	1.404
Cr_2O_3	0.1	0.000415	0.091	0.081	0.1	0.000235
Mn_2O_3	0.229	0.065	0.181	0.19	0.204	0.083
Fe_2O_3	14.972	3.384	8.912	6.321	6.997	1.514
ZnO	0.543	0.254	1.122	1.252	1.143	1.905
SrO	0.054	0.000318	0.06	0.081	0.093	0.091

supplementary cementitious materials (SCMs) to replace 20% of the OPC. The major chemical compositions (oxides) of three batches of MSWI ashes analyzed by X-ray Fluorescence (XRF) are shown in Tables 4.1, 4.2, and 4.3.

4.2.2. Treatment of the MSWI Samples. The MSWI materials were first collected and put into the oven under 105 °C for 24 hrs for drying, then put into a disc mill to grind with 700 rpm for 10mins to produce MSWI ashes. After that, 100 g ash and 200 g water were well mixed and sonicated with sonicator under 18 W for 5 mins to create a slurry for further treatment. The slurries were then put on a magnetic stirrer for constant mixing. Meanwhile, CO_2 was aerated into the slurries at the flow rate of 200 sccm, when pH meters were monitoring and recording the pH evolutions of the slurries. The aerating of CO_2 was remained on until the pH of the slurries reached ~6.6 and lasted for 10 mins.

4.2.3. Sample Preparation and Mix Design. The mix designs of the paste samples are shown in Table 4.4. For the paste samples with raw MSWI only, the replacement MSWI powder and the cement were first mixed for 3 mins, then added water and mixed. For upcycled samples, the treated MSWI slurries were used as the mixing water.

The mixed samples were cast into molds with the dimensions of 2cm×2cm×2cm, and the samples were covered with plastic film for the prevention of water evaporation. Then after 24 hrs, the samples were demolded and cured in the standard moisture curing room with 20 °C and RH>90% until the ages of compressive strength tests. The compressive strength tests were carried out on a hydraulic machine, and the most representative sample from each strength test was collected and put into small bottles

with isopropyl for stopping the hydration. After 24 hrs, the samples were removed from the bottles and put into the oven under 105 °C to dry for 1 d, and the dried samples were then ground into MSWI ashes with a disc mill.

Table 4.4 Mix design of MSWI samples

	Materials used for cement replacement	**Water (g)**	**OPC (g)**	**Cement Replacement (g)**
FA	Fly Ash	200	400	100
BA	Bottom Ash	200	400	100
SD	Sand	200	400	100
SA	Small Aggregate	200	400	100
FD	Ferrite Dirt	200	400	100
FC	Filter Cake	200	400	100
BA B+C	Bottom Ash + CO_2	200	400	100
SA+C	Small Aggregate + CO_2	200	400	100
FD+C	Ferrite Dirt + CO_2	200	400	100
SD+C	Sand + CO_2	200	400	100

4.2.4. Testing Procedures. The cube samples were tested with Tinus Olsen compressive strength tester. The paste cubes were first pre-loaded under 75 lbs for 10 s then loaded with the rate of 50 lbs per second until failure. For each mix at each age, five

samples were tested, and the average value was taken and went through the outlier analysis to get the representative strength.

The X-ray diffraction (XRD) tests were carried out for all the samples collected after the compressive tests. The powder samples were first dried, and the XRD diffractograms were collected by a PANanalytical X'pert Pro MPD diffractometer, using CuKα radiation (λ = 1.54 Å) and an X-Celerator solid detector. The step size was Δ2θ = 0.02626°, and the time per step was 200s.

4.3. RESULTS AND ANALYSIS

The testing results are listed and discussed in this section.

4.3.1. Composition Analysis of Raw MSWI Ashes. The oxide compositions of the three batches of MSWI ashes/fractions, determined by XRF, are shown in Figure 4.2. Detailed weight percentages of various oxides are listed in the tables in Section 4.2.1. The results show that all ash/fraction samples have relatively stable compositions. As potential alternative SCMs, the most critical oxides are SiO_2 and Al_2O_3. So herein, COVs of weight percentages of SiO_2 and Al_2O_3 – (COV_{SiO_2}, $COV_{Al_2O_3}$) – are used to measure the compositional stability of the samples. These two values of BA and FA are (0.05, 0.08) and (0.14, 0.11), respectively. As a reference, these two values for Class-F coal fly ash that is commonly used as an SCM in concrete are (0.10, 0.11). It suggests the stabilities of MSWI BA and FA are comparable to Class F coal fly ash.

Furthermore, when the fractions of BA were examined, it could be seen that all of them had comparable compositional stability to that of Class-F coal fly ash, except FC

had a large variation in the composition of SiO_2: FD (0.07, 0.13); SA (0.11, 0.04); SD (0.08, 0.07); and FC (0.18, 0.05).

The stabilities of MSWI ashes/fractions also imply that they can be supplied as potential SCMs for concrete production if the deleterious and toxic substances can be well managed.

4.3.2. The Treatment of MSWI Ashes. The MSWI ashes were treated by aerating CO_2 into their ash-water suspensions, for the sake of carbonation. The treatment data is shown in Table 4.5.

During the treatment of the MSWI powders, it was noticed that, different from the FD, SA, and FA ashes, parts of SD, FA, and BA ashes had lower densities than water, thereby floating on water. 21.4% and 34% of SD and BA were floating on water, respectively. FC had the largest percentage of 67.6% that floating on water. As shown in Figure 4.3, the portion of floating on water in BA ash has a large content of porous grains that have small particles absorbed in the pores. The floating part has a porous structure, which is very likely from the activated carbon that was added into the incinerator for the control of mercury and dioxins emissions. It implies that it contains mostly unburnt carbon. SA, FC and FA showed obvious CO_2 absorption, especially for FA, indicating different degree of reaction with CO_2, meaning the capability of upcycling with the CO_2-bubbling method, while other portions seem not to be upcycled with this method. In Figure 4.4, the XRD diffractogram of the BA ash floating on water indicates that there are some $CaCO_3$, SiO_2, $CaSO_4$, and NaCl absorbed in the porous carbon grain. Moreover, regarding BA sample, the floating part and the rests were separated and tested to

determine whether the top or bottom part has a more negative effect on the compressive strength of the paste samples in the Section 4.3.5.

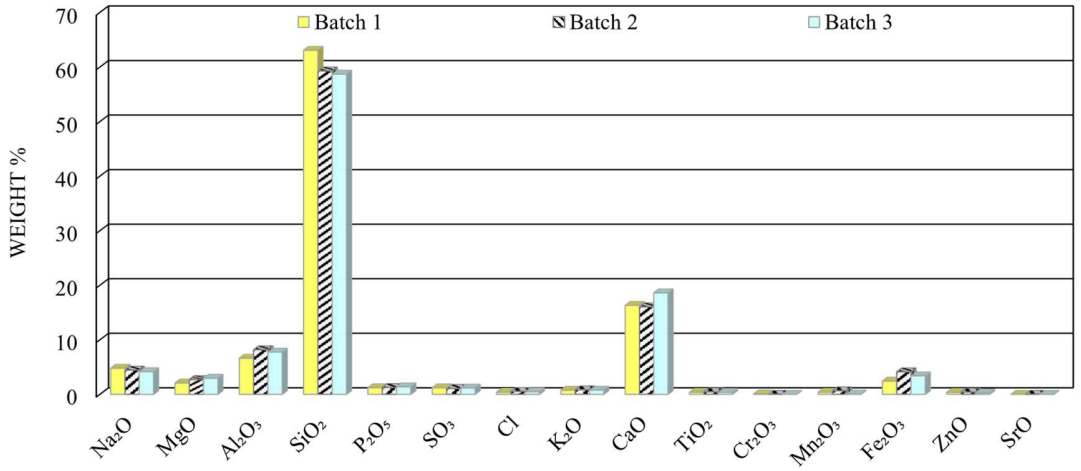

(a) FD

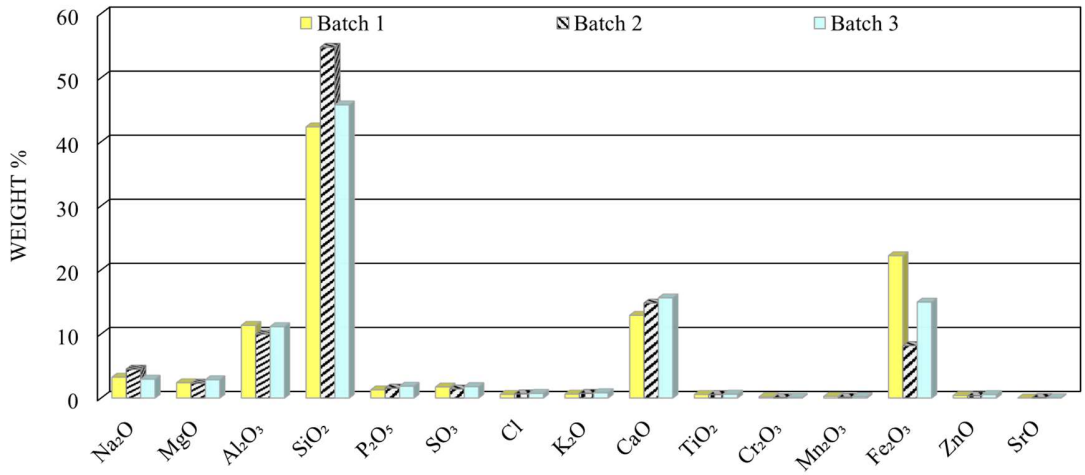

(b) SA

Figure 4.2 Comparisons of chemical compositions in the three batches of MSWI ashes. a) FD. b) SA. c) SD. (d) FC. (e) BA. (f) FA. and (g) Average of the three batches.

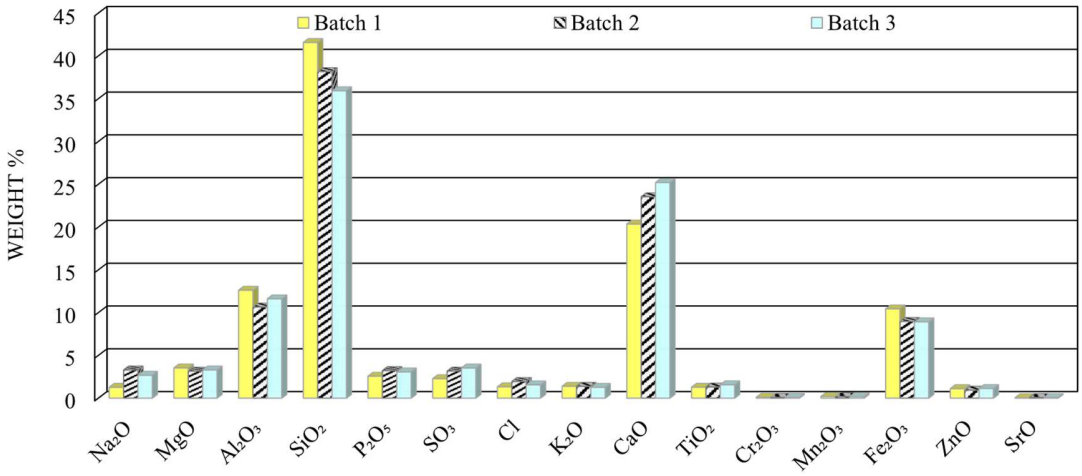

(c) SD

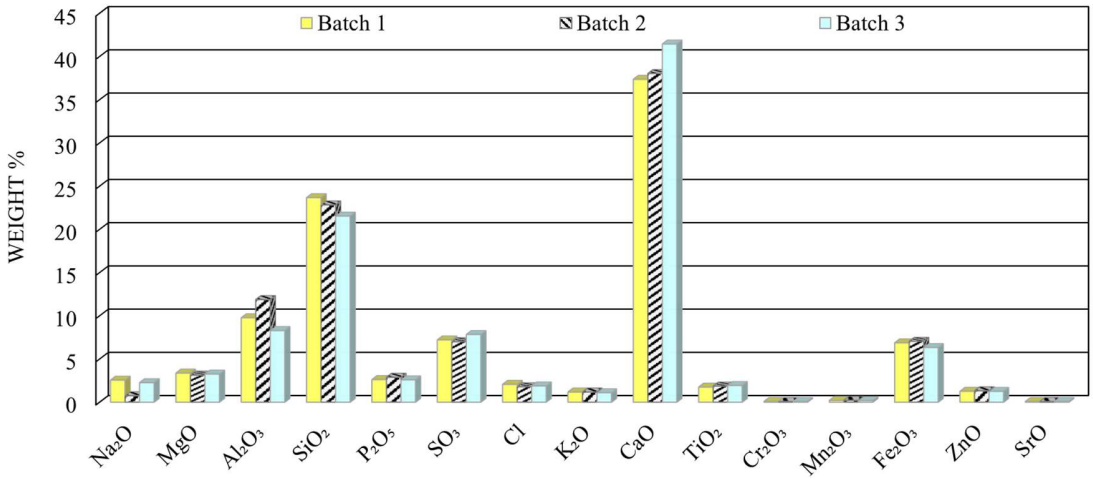

(d) FC

Figure 4.2 Comparisons of chemical compositions in the three batches of MSWI ashes. a) FD. b) SA. c) SD. (d) FC. (e) BA. (f) FA. and (g) Average of the three batches. (Cont.)

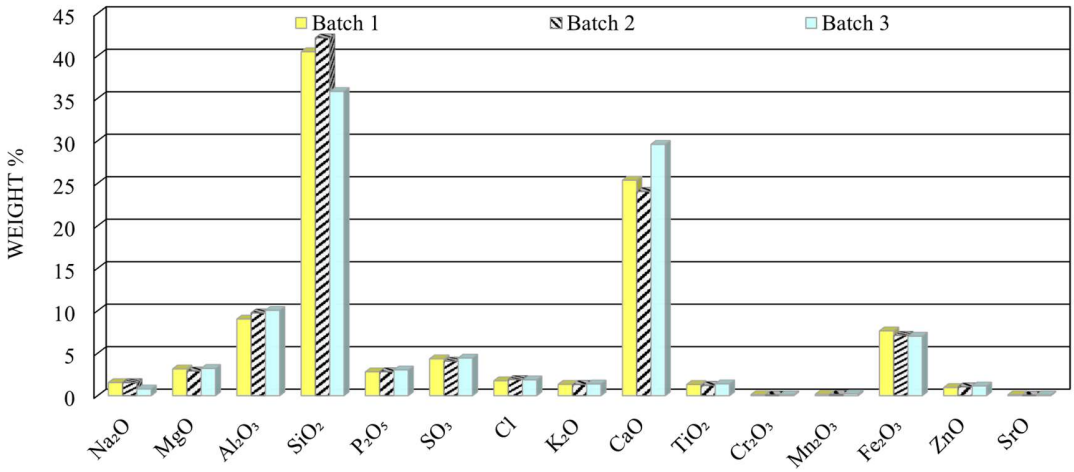

(e) BA

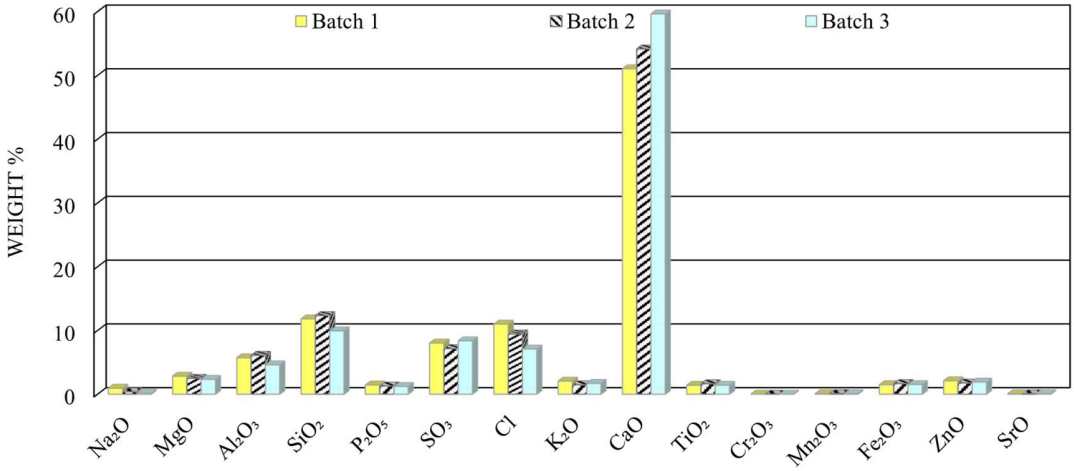

(f) FA

Figure 4.2 Comparisons of chemical compositions in the three batches of MSWI ashes. a) FD. b) SA. c) SD. (d) FC. (e) BA. (f) FA. and (g) Average of the three batches. (Cont.)

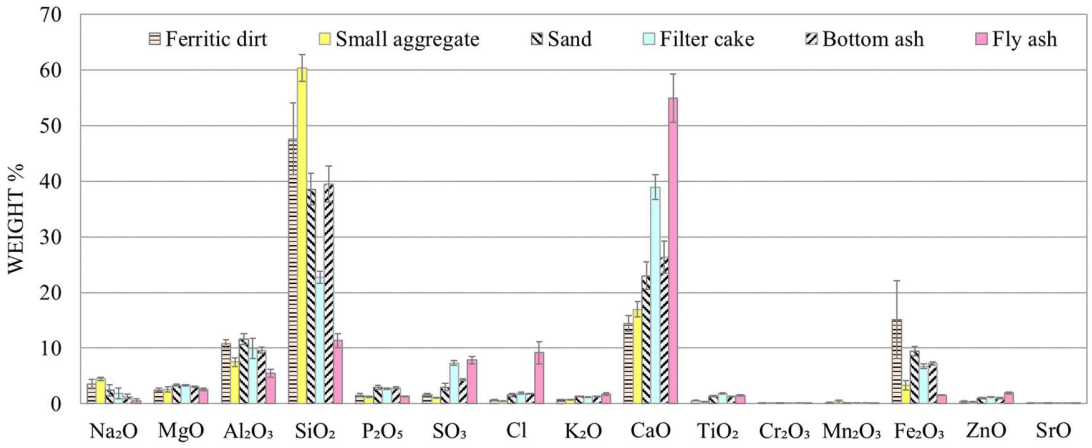

(g) Average

Figure 4.2 Comparisons of chemical compositions in the three batches of MSWI ashes. a) FD. b) SA. c) SD. (d) FC. (e) BA. (f) FA. and (g) Average of the three batches. (Cont.)

4.3.3. The Workability of the Fresh Paste and the Morphology of the Hardened Cubes.

Different MSWI powders had different effects on the workability of the fresh cement paste, compared to the control groups: 1. Samples with FA had normal consistency; 2. Samples with BA, FC, and SD all showed thicker consistency than the OPC samples, after the paste was casted and leveled in the molds, they all showed major expansion; 3. Samples with FD and SA had smoother consistency while mixing, the cement pastes were fairly liquid after mixing.

Moreover, at the early hydration stage of the fresh cement pastes with BA, SD, FC, and FD ashes, there are some gases released from the pastes, generating some bubbles after pastes were casted into the molds. This can be attributed to the existence of metallic aluminum in these MSWI ashes (see the XRD test results in Figure 4.5), which will react with water under a high pH environment and release hydrogen gas.

Table 4.5 Treatment data of MSWI ash samples

Sample	Initial weight (g)	Starting pH	Amount with lower density (g)	Amount with higher density (g)	CO_2 absorption (g)
FD	100	10.2	-	100	-
SA	100	9.8	-	100	0.1
SD	100	10.5	21.4	78.6	-
FC	100	10.9	67.6	32.4	0.1
BA	100	10.6	34	66	-
FA	100	12.1	-	100	0.5

As for the hardened paste samples, it was found that the paste with unsorted BA had a volume expansion and did not have volume stability as good as the paste with FA, as shown in Figure 4.6.

When investigating the pastes with the four fractions of BA, paste samples with SA had little volume change and were in a good regular shape, while the pastes with BA, FC, and SD had major expansions, leading to swelling of their top surfaces, along with the presence of voids due to the gas released at the early hydration stage. In addition, the samples with BA, FC, and SD showed a darker color due to the higher contents of unburned carbon, and the samples with FD and SA appeared to be lighter in color.

4.3.4. The Evolvement of Hydration Heat. The heat flow rate curves and the cumulative heat flow curves of the cement pastes with the batch 1 MSWI ashes are

shown in Figure 4.7. As manifested in Figure 4.7(a), the cumulative heat of OPC is the lowest among all the samples, which means the partially (i.e., 20%) replacements of cement by the MSWI ashes have an augmenting effect on the hydration heat released of OPC. Additionally, FA samples have an acceleration effect on cement hydration. It can also be seen from Figure 4.7(b) that the first heat flow peaks of the FA-Paste samples come much earlier than that of the control group. For pastes with other MSWI ashes, the heat releasing rates of the first hydration peaks do not vary a lot, but their accumulated hydration heats are higher than that of the control group. So, it is clear that the MSWI ashes will fortify the hydration heat released by the paste, and FA ashes can also have an acceleration effect on the hydration of cement paste.

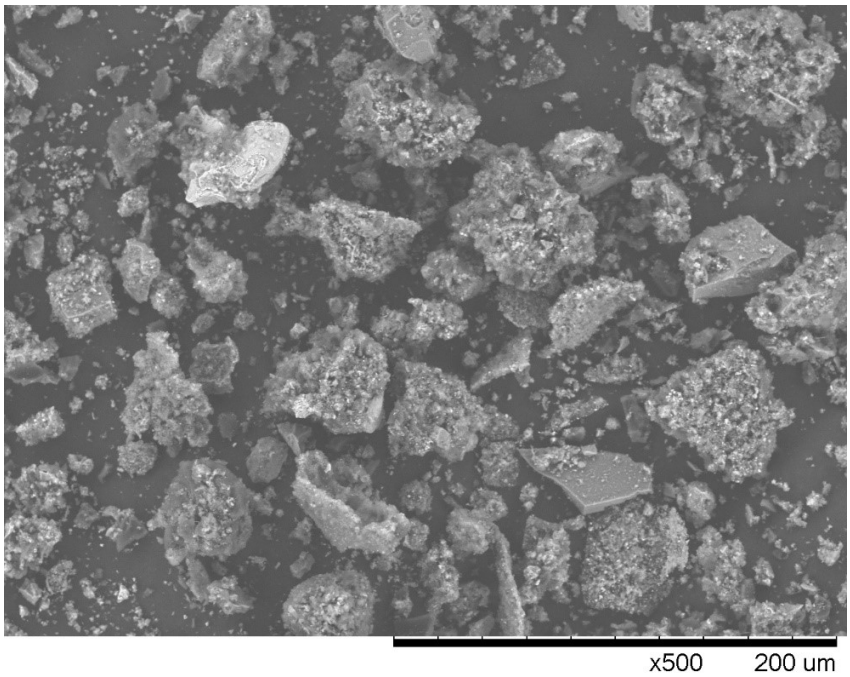

Figure 4.3 Micro-structure of the portion of BA ash that floating on water.

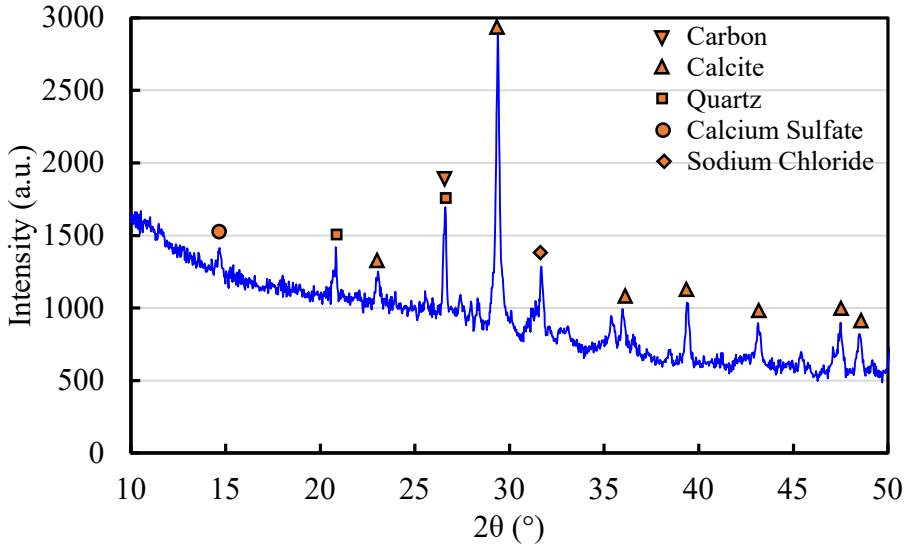

Figure 4.4 XRD diffractogram of the portion of BA ash that floating on water.

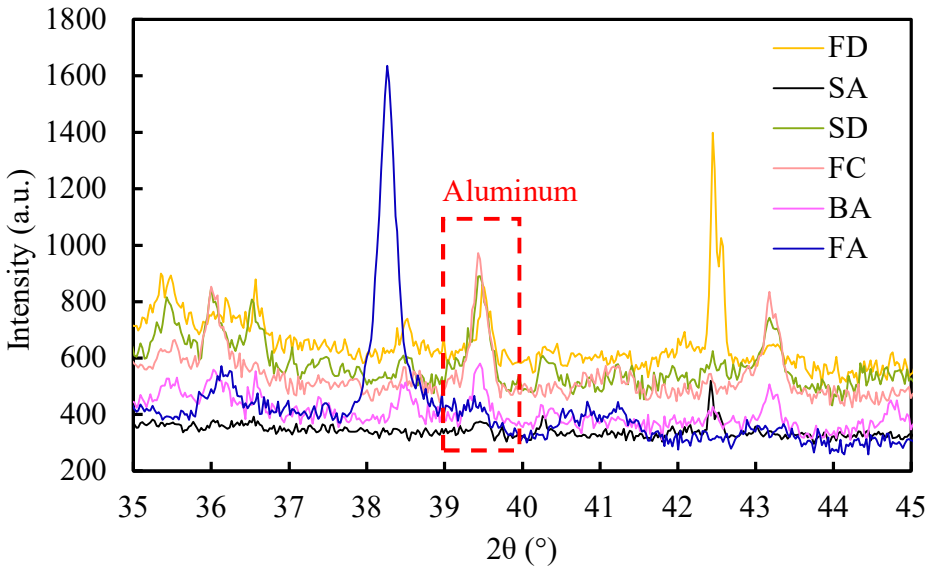

Figure 4.5 Aluminum peaks in the XRD results of the six MSWI ashes.

4.3.5. The Development of Compressive Strength. Before the carbonation treatment of the three batches of MSWI ashes, the compressive strengths of the paste samples with untreated MSWI ashes were evaluated, exhibited in Figure 4.8. According to the figures, there is a negative effect on the compressive strength after 20% cement replacement by MSWI ashes in the cement pastes, compared to the control group without cement replacement. The FA samples in each batch showed the least deterioration effect, reached about 80% of the compressive strength of the control group at later ages (i.e., 56 days), while the BA samples had the lowest strength among all the samples. The compressive strengths of MSWI paste samples showed similar trends among all three batches, albeit the FC samples in the second batch had a more significant decrease in the compressive strength of the paste samples compared to the other two batches. This could

Figure 4.6 Photos of cement pastes incorporating (from left to right): FA, BA, SA, SD, FC, and FD.

be ascribed to the fact that the FC from the second batch had a higher content of alumina or metallic aluminum than those from the first and third batches, according to the chemical composition tables in Tables 4.1, 4.2, and 4.3.

After the MSWI ashes were treated by CO_2-bubbling method, the compressive strengths of the cement pastes incorporated with the treated MSWI ashes (i.e., BA, SA, FD, and SD) were explored, as displayed in Figure 4.9. FC was excluded in the strength study due to its high variation of silica content and its large portion with unburned carbon), as suggested in Section 4.3.1 and Table 4.3. According to Figure 4.9, after the MSWI ashes are treated with carbonation, all paste groups incorporated with treated BAB, SA, FD and SD ashes showed different increments in compressive strengths, and the enhancements are throughout all curing ages. The strength of the paste sample with SA+C ashes is twice as strong as that of the paste with SA ashes.

It is noticed that the bottom part of BA (BAB) has a more deterioration effect on the compressive strength than the original BA, as shown in Figure 4.9. Since the BAB has less unburnt carbon but more aluminum than the portion floating on water, it suggests the aluminum is the reason that is dominant in the strength depression of paste with BA ashes, in comparison with the curtailment of strength from unburnt carbon.

XRD tests were carried out on the paste samples with treated and untreated BAB or BA ashes at an early age (i.e., 1 day), as shown in Figure 4.10. The paste samples with carbonation-treated MSWI ashes have apparently more $CaCO_3$ than the paste samples with untreated MSWI ashes. The excess $CaCO_3$ is rooted in the carbonation treatment of MSWI ashes. In Figure 4.11, the microstructures of treated BA ash grains and the calcite particles produced amid carbonation treatment are presented.

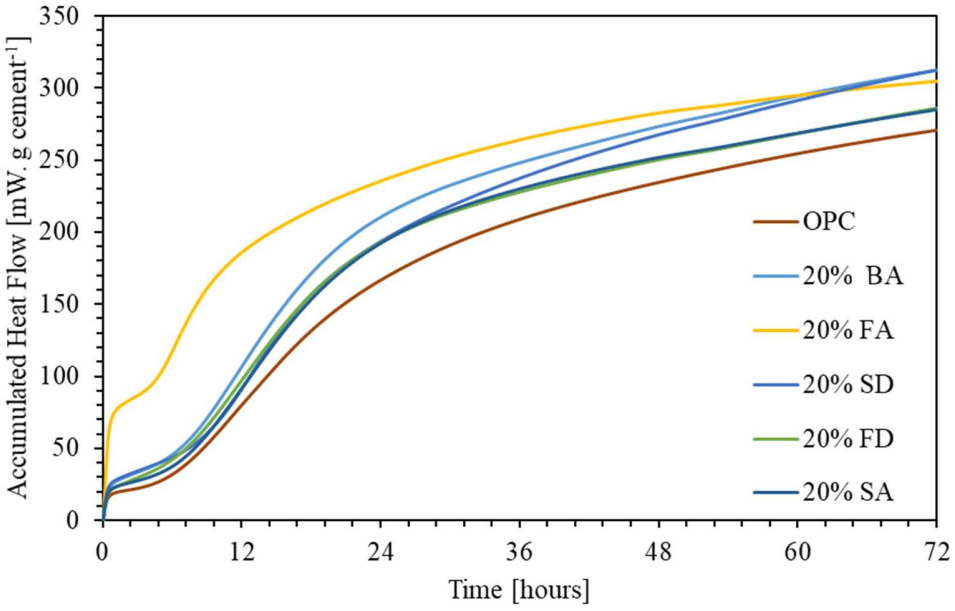

(a)

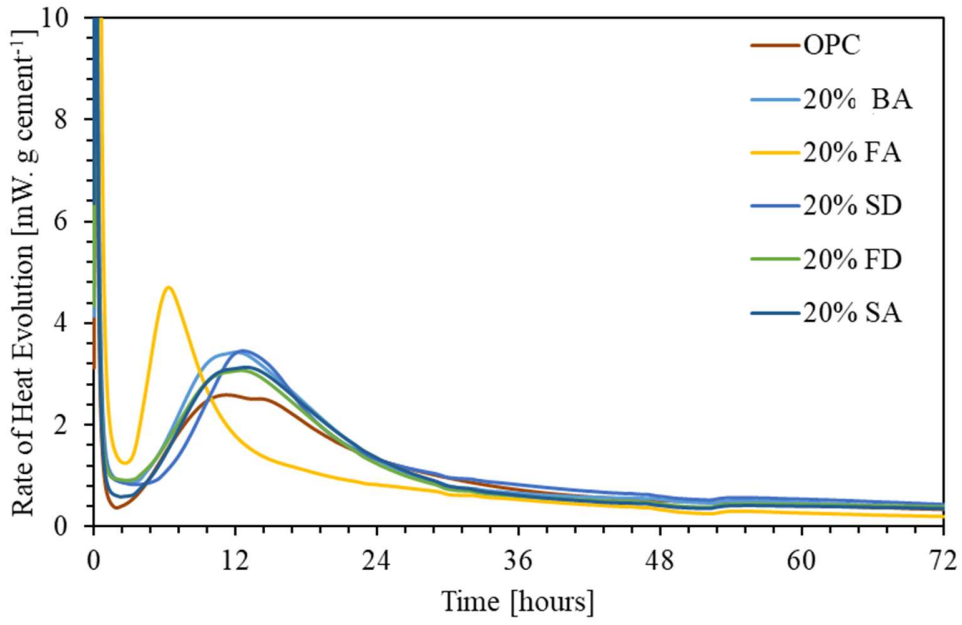

(b)

Figure 4.7 Evolvements of hydration heat of pastes incorporated with MSWI ashes. a) Cumulative heat released. b) Heat flow rate released.

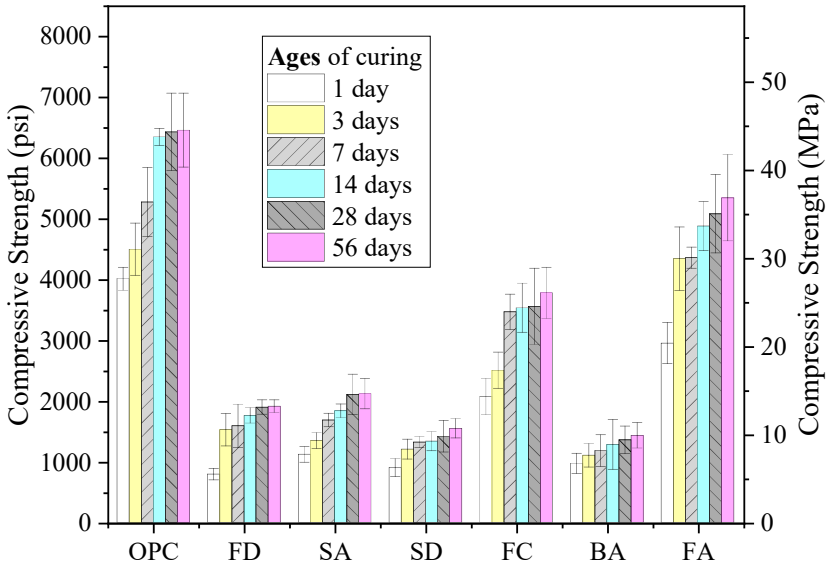

(a)

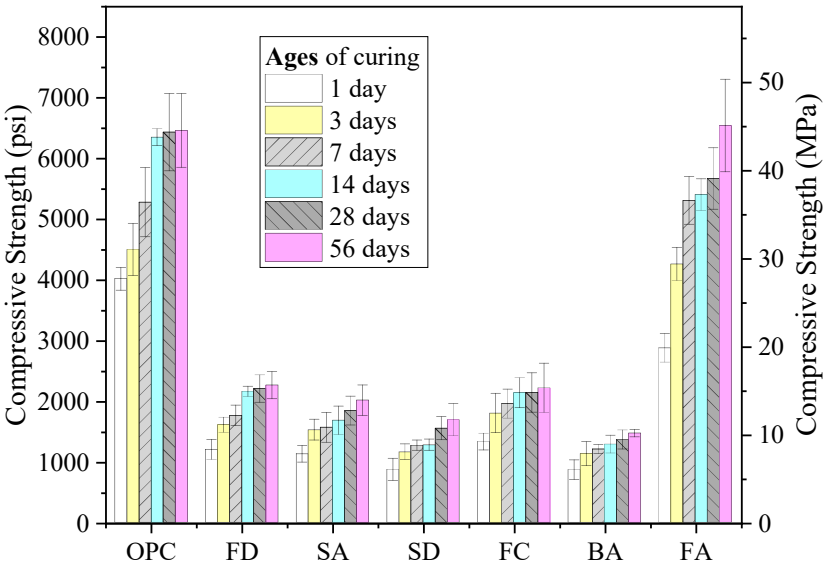

(b)

Figure 4.8 Compressive strengths of the cement paste samples with the three batches of untreated MSWI ashes. a) Batch 1. b) Batch 2. c) Batch 3.

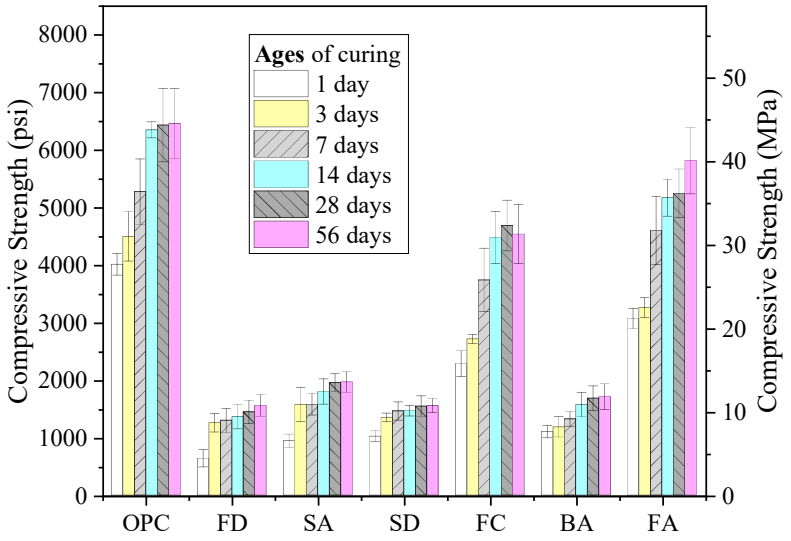

(c)

Figure 4.8 Compressive strengths of the cement paste samples with the three batches of untreated MSWI ashes. a) Batch 1. b) Batch 2. c) Batch 3(Cont)

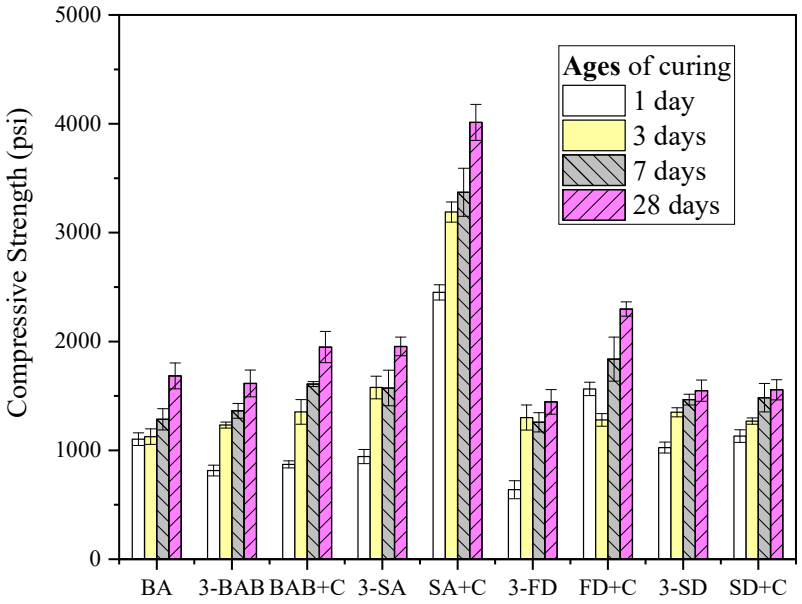

Figure 4.9 Compressive strength of MSWI ash paste samples at various ages, w/c = 0.4.

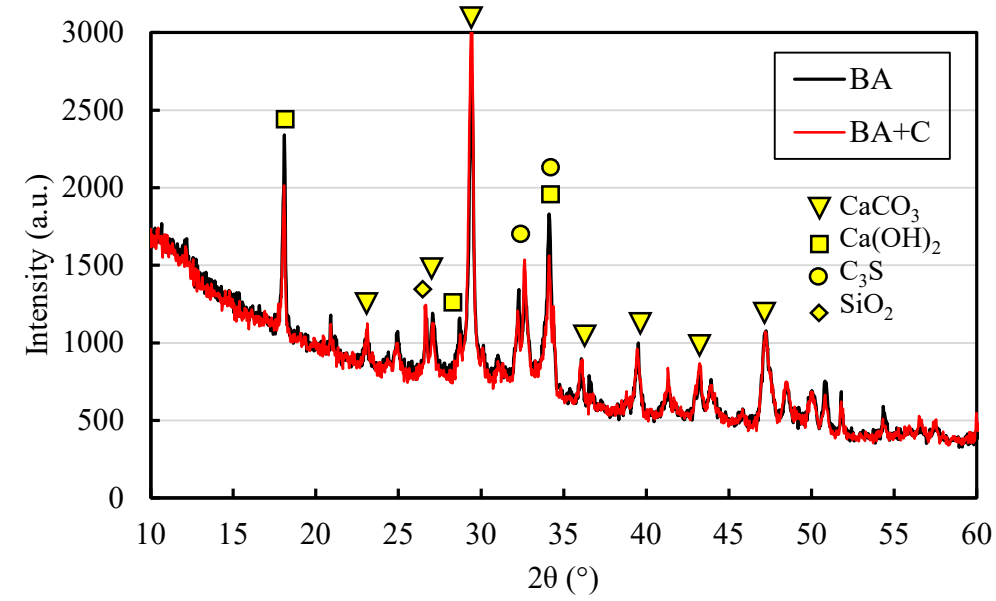

(a)

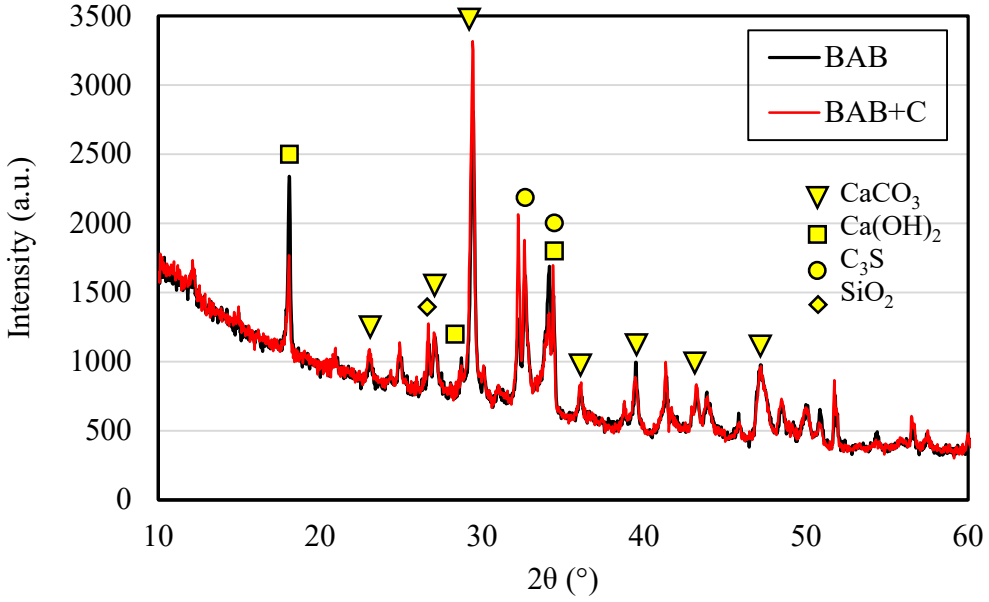

(b)

Figure 4.10 XRD test result of 1-day paste samples with carbonation-treated and untreated BA(a) or BAB(b) ashes

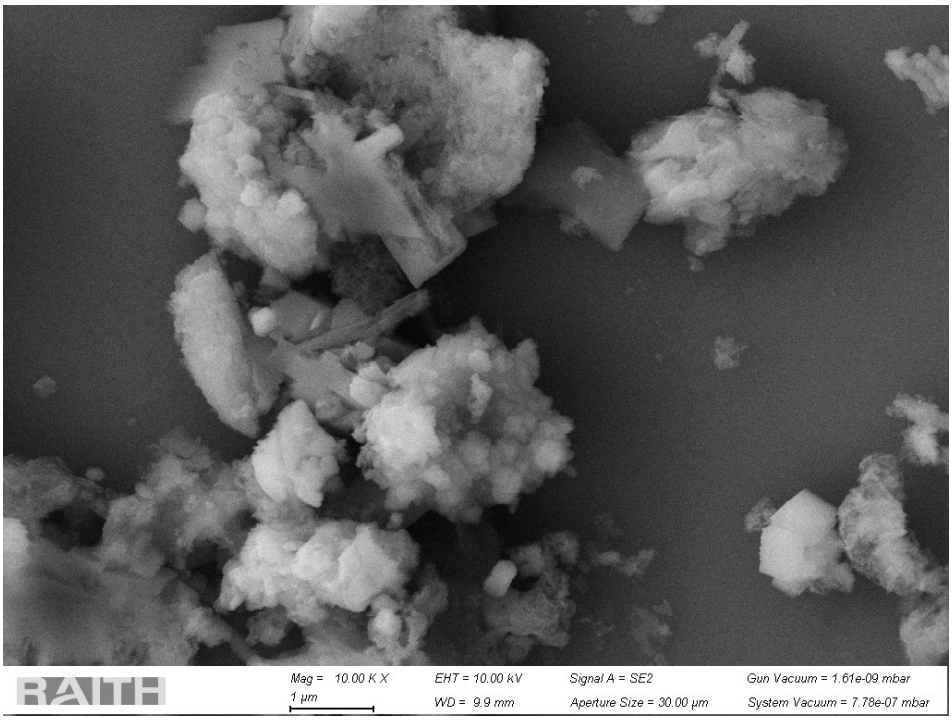

(a)

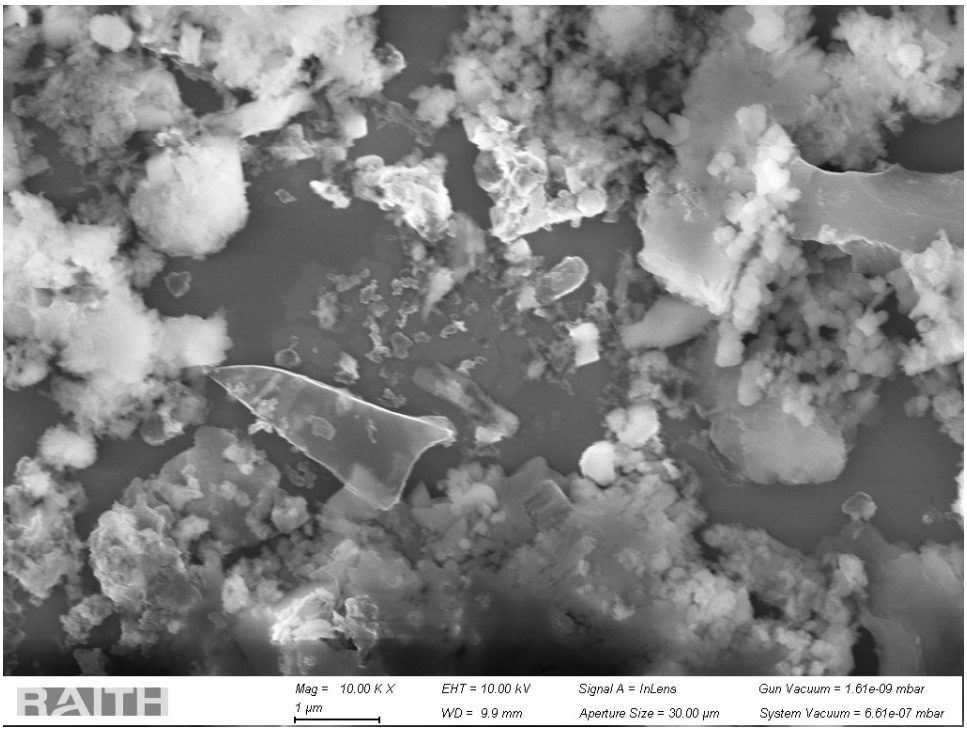

(b)

Figure 4.11 SEM images of the carbonation-treated BA ashes: (a) ash grains, (b) cluster of particles generated after carbonation treatment.

4.4. DISCUSSION

The MSWI FA, BA, and BA fractions have shown their potentials to be upcycled into alternative SCMs or into construction products directly. However, how to effectively mitigate the adverse effects of unburned carbon and metallic aluminum, as well as to evaluate the ashes' potential as SCMs more accurately, need to be figured out.

A large portion of unburned carbon can be separated by mechanical agitation and rest since it has a lower density than water. In this study, we have also preliminarily demonstrated that carbonation-treatment of the MSWI ash in the diluted suspension could improve the compressive strength of ash-incorporated cement paste, though the metallic aluminum had not been removed. As revealed by Heuss-Aßbichler et al. [196] the metallic aluminum is wrapped in glassy phases in the BA fractions, which explains why the aluminum could not be recovered by Eddy current. Grinding of the BA fractions will expose the aluminum, so adding lime in the above-mentioned diluted suspension could effectively convert the aluminum. If desired, a device can be designed to collect hydrogen gas released in this process.

Once the above issues (unburned carbon and aluminum) are addressed in the diluted suspension, the processed ashes can be filtered out to be alternative SCMs or to mix into construction materials directly. The optimal and maximum dosages of them in making cement-based materials can be investigated furtherly to establish experimental protocols.

4.5. CONCLUSIONS

From the tests presented in this study, the following conclusions can be drawn:

(1) the MSWI ashes/fractions have comparable good compositional stabilities to the conventional SCM of Class-F coal fly ash, implying that they can be supplied as potential SCMs for concrete production. An exception is the FC fraction has a much larger fluctuation in silica content and a high content of unburned carbon, which was excluded in the strength test in this study.

(2) Different MSWI ashes/fractions have different effects on the workability of the fresh cement paste. The swelling phenomenon and gas released in the early hydration stage can be attributed to the existence of metallic aluminum in these MSWI ashes, which will react with water under a high pH environment and release hydrogen gas.

(3) The unburned carbon in the MSWI ashes has a porous structure and a lower density than water, so it is floating on water. No floating portions were found in the suspensions of FA, FD, and SA ashes. However, the SD, FC, and BA ashes have relatively large portions floating on water, indicating higher unburned carbon contents.

(4) Different MSWI ashes/fractions show different CO_2 absorption, indicating the capability of the upcycling with the CO_2-bubbling method.

(5) The untreated MSWI ashes have a negative effect on the compressive strength of cement pastes, mainly due to the unburned carbon and the metallic aluminum. Moreover, aluminum has a more severe impact on the strength development than unburned carbon.

(6) After the MSWI ashes are treated by the CO_2-bubbling method, the compressive strengths of the ash-incorporated pastes can be improved

apparently, especially for the SA samples, which matches the CO_2 absorption. It manifests the effectiveness of the carbonation treatment method on the improvement of the compressive strength of the ash-incorporated cement pastes.

5. SUMMARY AND CONCLUSION

Summarizing the experimental results, the following conclusions can be drawn:

The *in situ* synthesis of calcium carbonate under room temperature with CO_2 bubbling method is able to produce nano-sized calcite particles, the produced nano-calcite suspension can be used as mixing water to prepare cement-based materials:

(1) The particle size of calcite particles can be influenced by the concentration of the CH slurries: generally, the average particle size is decreasing with the increase of the concentration of CH. The morphologies of the particles vary from rice-shaped to spindle-shaped, with the average particle size below 1μm. Agglomeration is detected.

(2) The addition of superplasticizer can influence the particle distribution; thus, the particle size distribution can be benefited by the introduction of superplasticizer, and the agglomeration can be mitigated by superplasticizer.

(3) The nano-calcite suspension can be used as the mixing water to prepare cement-based materials. The nano-calcite in the suspension act as a traditional accelerator that provides high early-age (i.e., up to an age of 7 days) compressive strength, and the acceleration effect is increasing with the increase of the concentration of nano-calcite, especially for the superplasticizer groups.

(4) The addition of superplasticizer can enhance the overall compressive strength by providing a better particle distribution for the nano-calcite.

MSWI ashes provided by York County are separated, characterized, and tested for the basic properties, then the ashes are treated with CO_2-bubbling method and used as SCM to prepare cement pastes:

(1) The composition of the MSWI ashes have compositional stabilities good enough to be used as SCM for concrete production.

(2) SA, FC, and FA show better CO_2 absorption, indicating the potential of being upcycled with CO_2-bubbling method.

(3) The MSWI ashes have negative effects on the compressive strength of cement paste when added as SCM due to the high content of unburnt carbon and metallic aluminum, and metallic aluminum has more severe impact on the compressive strength.

(4) The upcycling of MSWI ashes is proved to improve the compressive strength of the MSWI ash-incorporated pastes, especially for the samples with SA, the one ash with high CO_2 absorption during upcycling.

Above all, the *in situ* carbonation method is proved to produce nano-sized calcite particle, with the incorporation of superplasticizer, the morphology and size of the particle can be optimized. The upcycling of MSWI ashes with CO_2-bubbling method produced a promising result, the samples with high CO_2 absorption capability showed a ~100% compressive strength increase at all stages, indicating a potential of becoming ASCM that could provide sufficient strength for the structures.

The feasibility of the *in situ* upcycle with CO_2-bubbling method is also proved. Since the formation of nano-calcite requires a calcium source, some industrial solid wastes with high calcium content could possibly be the ideal candidate for this method. Also, the utilization with CO_2-rich flue gas from industries as the carbon source for the upcycle could be another route for reducing the carbon emission.

Furthermore, this study mainly focuses on the feasibility of the CO_2-bubbling method for synthesizing nano-calcite under room temperature and for upcycling the MSWI ashes, the mechanism for the upcycling and the possible influences of other cementitious additives on the nano-calcite synthesis is still remain investigating.

BIBLIOGRAPHY

[1] T. Oda, S. Maksyutov, and R. J. Andres, "The Open-source Data Inventory for Anthropogenic CO2, version 2016 (ODIAC2016): a global monthly fossil fuel CO2 gridded emissions data product for tracer transport simulations and surface flux inversions," *Earth Syst. Sci. Data,* vol. 10, no. 1, pp. 87-107, 2018, doi: 10.5194/essd-10-87-2018.

[2] P. C. Jain, "Greenhouse effect and climate change: scientific basis and overview," *Renewable Energy,* vol. 3, no. 4, pp. 403-420, 1993/06/01/ 1993, doi: https://doi.org/10.1016/0960-1481(93)90108-S.

[3] H. Ritchie and M. Roser, "CO2 emissions ", ed, 2020.

[4] N. O. a. A. Administration, "Trends in atmospheric carbon dioxide," ed, 2021.

[5] G. S. Dwyer and M. A. Chandler, "Mid-Pliocene sea level and continental ice volume based on coupled benthic Mg/Ca palaeotemperatures and oxygen isotopes," *Philosophical Transactions of the Royal Society A: Mathematical, Physical and Engineering Sciences,* vol. 367, no. 1886, pp. 157–168, 2009.

[6] D. J. Lunt, A. M. Haywood, G. L. Foster, and E. J. Stone, "The Arctic cryosphere in the Mid-Pliocene and the future," *Philosophical Transactions of the Royal Society A: Mathematical, Physical and Engineering Sciences,* vol. 367, no. 1886, pp. 49-67, 2009.

[7] K. Ricke and K. Caldeira, "Maximum warming occurs about one decade after a carbon dioxide emission," *Environmental Research Letters,* vol. 9, no. 12, p. 124002, 2014.

[8] G. L. Foster and E. J. Rohling, "Relationship between sea level and climate forcing by CO2 on geological timescales," *Proceedings of the National Academy of Sciences of the United States of America (PNAS),* vol. 110, no. 4, pp. 1209-1214, 2013.

[9] O. D. B. Metz, H.C. De Coninck, M. Loss, L.A. Meyer, "IPCC Special Report on Carbon Dioxide Capture and Storage," p. 442, 2005. Cambridge University Press,.

[10] C. D. Thomas *et al.*, "Extinction risk from climate change," *Nature,* vol. 427, no. 6970, pp. 145-148, 2004/01/01 2004, doi: 10.1038/nature02121.

[11] T. W. House, "Fact Sheet: President Biden Sets 2030 Greenhouse Gas Pollution Reduction Target Aimed at Creating Good-Paying Union Jobs and Securing U.S. Leadership on Clean Energy Technologies," The White House Briefing Room, Washington DC, 2021.

[12] P. Cavaliere, *Clean ironmaking and steelmaking processes*. Springer Nature Switzerland AG, 2019.

[13] ASCE, " 2017 Infrastructure Report Card," ed: American Society of Civil Engineers, 2017.

[14] K. L. Scrivener, V. M. John, and E. M. Gartner, "Eco-efficient cements: Potential economically viable solutions for a low-CO2 cement-based materials industry," *Cement and Concrete Research,* vol. 114, pp. 2-26, 2018.

[15] T. Boden and B. Andres, "Global CO2 Emissions from Fossil-Fuel Burning, Cement Manufacture, and Gas Flaring: 1751-2014," Oak Ridge National Laboratory, Oak Ridge, Tennessee, USA, 2017.

[16] M. Schneider, "Process technology for efficient and sustainable cement production," *Cement and Concrete Research,* vol. 78, no. Part A, pp. 14-23, 2015.

[17] M. C. G. Juenger, F. Winnefeld, J. L. Provis, and J. H. Ideker, "Advances in alternative cementitious binders," *Cement and Concrete Research,* vol. 41, pp. 1232-1243, 2011.

[18] N. Xie, X. Shi, Y. Dang, and A. Pace, "Upcycling of waste materials: green binder prepared with pure coal fly ash," *Journal of Materials in Civil Engineering,* vol. 28, no. 3, p. 04015138, 2016.

[19] ACAA, "2016 Coal Combustion Product (CCP) Production & Use Survey Report," American Coal Ash Association, Farmington Hills, MI, 2017.

[20] A. C. A. Association, "2014 Coal Combustion Product (CCP) Production & Use Survey Report," Farmington Hills, MI, 2014.

[21] WBCSD, "Cement Sustainability Initiative, Getting the Numbers Right, Project Emissions Report 2014," http://www.gnr-project.org/, 2016.

[22] LC3, "Limestine calcined clay cement," ed: LC3 Project Office, 2014.

[23] M. Antoni, J. Rossen, F. Martirena, and K. Scrivener, "Cement substitution by a combination of metakaolin and limestone," *Cement and Concrete Research,* vol. 42, pp. 1579–1589, 2012.

[24] R. Snellings, "Assessing, Understanding and Unlocking Supplementary Cementitious Materials," *RILEM Technical Letters,* vol. SI 1, pp. 50–55, 2016.

[25] W. Fung, A. Kwan, and H. Wong, "Wet packing of crushed rock fine aggregate," *Materials and Structures* vol. 42, no. 5, pp. 631-643, 2009.

[26] E. Berodier and K. Scrivener, "Understanding the Filler Effect on the Nucleation and Growth of C‐S‐H," *Journal of the American Ceramic Society* vol. 97, no. 12, pp. 3764-3773, 2014.

[27] F. Sanchez and K. Sobolev, "Nanotechnology in concrete-A review," *Construction and Building Materials,* vol. 24, no. 11, pp. 2060-2071, 2010.

[28] P. Aïtcin and R. Flatt, *Science and Technology of Concrete Admixtures*. Woodhead Publishing, 2016.

[29] J. Péra and J. Ambroise, "New applications of calcium sulfoaluminate cement," *Cement and Concrete Research,* vol. 34, no. 4, pp. 671-676, 2004.

[30] K. Scrivener "Calcium aluminate cements," in *Advanced Concrete Technology*, J. Newman and B. S. Choo, Eds. Burlington, MA: Butterworth-Heinemann, 2003.

[31] M. Juenger, F. Winnefeld, J. Provis, and J. Ideker, "Advances in alternative cementitious binders," *Cement and Concrete Research* vol. 41, no. 12, pp. 1232-1243, 2011.

[32] X. Ke, S. Bernal, and J. Provis, "Assessing the long-term structural changes of metakaolin geopolymers encapsulating strontium loaded ion-exchanger," in *International Conference on Alkali Activated Materials and Geopolymers: Versatile Materials Offering High Performance and Low Emissions*, 2018.

[33] J. Provis and S. Bernal, "Geopolymers and Related Alkali-Activated Materials," *Annual Review of Materials Research,* vol. 44, pp. 299-327, 2014.

[34] J. Provis and J. van Deventer, *Alkali activated materials: state-of-the-art report, RILEM TC 224-AAM*. Springer, 2013.

[35] F. Xi *et al.*, "et al. Substantial global carbon uptake by cement carbonation," *Nature Geoscience,* vol. 9, pp. 880-883, 2016.

[36] D. Zhang, Z. Ghouleh, and Y. Shao, "Review on carbonation curing of cement-based materials," *Journal of CO_2 Utilization,* vol. 21, pp. 119-131, 2017.

[37] V. Rostami, Y. Shao, A. Boyd, and Z. He, "Microstructure of cement paste subject to early carbonation curing," *Cement and Concrete Research,* vol. 42, no. 1, pp. 186-193, 2012.

[38] CarbonCure, "CarbonCure Technologies Inc.," ed.

[39] M. Thomas, "Impact of CO2 Utilization in Fresh Concrete on Corrosion of Steel Reinforcement," CarbonCure Technologies Inc., Dartmouth, NS, Canada, 2019.

[40] Z. Wei *et al.*, "Clinkering-free cementation by fly ash carbonation," *Journal of CO2 Utilization,* vol. 23, pp. 117-127, 2018.

[41] S. A. Walling and J. L. Provis, "Magnesia-based cements: A journey of 150 years, and cements for the futher?," *Chemical Reviews,* vol. 116, p. 4170−4204, 2016.

[42] Solidia, "Solidia," ed.

[43] CarbiCrete, "CarbiCrete," ed.

[44] M. Ni and B. D. Ratner, "Differentiating calcium carbonate polymorphs by surface analysis techniques—an XPS and TOF-SIMS study," *Surface and Interface Analysis,* vol. 40, no. 10, pp. 1356-1361, 2008/10/01 2008, doi: 10.1002/sia.2904.

[45] M. Maslehuddin, A. M. Sharif, M. Shameem, M. Ibrahim, and M. S. Barry, "Comparison of properties of steel slag and crushed limestone aggregate concretes," *Construction and Building Materials,* vol. 17, no. 2, pp. 105-112, 2003/03/01/ 2003, doi: https://doi.org/10.1016/S0950-0618(02)00095-8.

[46] A. M. Alhozaimy, "Effect of absorption of limestone aggregates on strength and slump loss of concrete," *Cement and Concrete Composites,* vol. 31, no. 7, pp. 470-473, 2009/08/01/ 2009, doi: https://doi.org/10.1016/j.cemconcomp.2009.04.010.

[47] J. Péra, S. Husson, and B. Guilhot, "Influence of finely ground limestone on cement hydration," *Cement and Concrete Composites,* vol. 21, no. 2, pp. 99-105, 1999/04/01/ 1999, doi: https://doi.org/10.1016/S0958-9465(98)00020-1.

[48] A.-M. Poppe and G. De Schutter, "Cement hydration in the presence of high filler contents," *Cement and Concrete Research,* vol. 35, no. 12, pp. 2290-2299, 2005/12/01/ 2005, doi: https://doi.org/10.1016/j.cemconres.2005.03.008.

[49] M. Cao, C. Zhang, H. Lv, and L. Xu, "Characterization of mechanical behavior and mechanism of calcium carbonate whisker-reinforced cement mortar," *Construction and Building Materials,* vol. 66, pp. 89-97, 2014/09/15/ 2014, doi: https://doi.org/10.1016/j.conbuildmat.2014.05.059.

[50] J. Pan, J. Cai, H. Ma, and C. K. Y. Leung, "Development of Multiscale Fiber-Reinforced Engineered Cementitious Composites with PVA Fiber and CaCO3 Whisker," *Journal of Materials in Civil Engineering,* vol. 30, no. 6, p. 04018106, 2018, doi: doi:10.1061/(ASCE)MT.1943-5533.0002305.

[51] L. Li and M. Cao, "Influence of calcium carbonate whisker and polyvinyl alcohol-steel hybrid fiber on ultrasonic velocity and resonant frequency of cementitious composites," *Construction and Building Materials,* vol. 188, pp. 737-746, 2018/11/10/ 2018, doi: https://doi.org/10.1016/j.conbuildmat.2018.08.154.

[52] M. Cao, L. Li, C. Zhang, and J. Feng, "Behaviour and damage assessment of a new hybrid-fibre-reinforced mortar under impact load," *Magazine of Concrete Research,* vol. 70, no. 17, pp. 905-918, 2018, doi: 10.1680/jmacr.16.00536.

[53] D. Wang, C. Shi, N. Farzadnia, Z. Shi, H. Jia, and Z. Ou, "A review on use of limestone powder in cement-based materials: Mechanism, hydration and microstructures," *Construction and Building Materials,* vol. 181, pp. 659-672, 2018/08/30/ 2018, doi: https://doi.org/10.1016/j.conbuildmat.2018.06.075.

[54] I. M. A.-N. America. "What is calcium carbonate?" Industrial Minerals Association - North America. https://www.ima-na.org/page/what_is_calcium_carb (accessed 9/10, 2021).

[55] T. Nypelö, M. Österberg, and J. Laine, "Tailoring Surface Properties of Paper Using Nanosized Precipitated Calcium Carbonate Particles," *ACS Applied Materials & Interfaces,* vol. 3, no. 9, pp. 3725-3731, 2011/09/28 2011, doi: 10.1021/am200913t.

[56] J. Ebrahimpour Kasmani, S. Mahdavi, A. Alizadeh, M. Nemati, and A. Samariha, "Physical Properties and Printability Characteristics of Mechanical Printing Paper with LWC," *2013,* Scanning microscope; Precipitated calcium carbonate; Nanoclay; Surface picking; Printability vol. 8, no. 3, p. 11, 2013-05-23 2013. [Online]. Available: https://ojs.cnr.ncsu.edu/index.php/BioRes/article/view/BioRes_08_3_3646_Ebrahimpour_Printability_Characteristics.

[57] K. Piekarska, P. Sowinski, E. Piorkowska, M. M. U. Haque, and M. Pracella, "Structure and properties of hybrid PLA nanocomposites with inorganic nanofillers and cellulose fibers," *Composites Part A: Applied Science and Manufacturing,* vol. 82, pp. 34-41, 2016/03/01/ 2016, doi: https://doi.org/10.1016/j.compositesa.2015.11.019.

[58] V. T. Nguyen, J.-c. Lee, J. Jeong, B.-S. Kim, G. Cote, and A. Chagnes, "Extraction of Gold(III) from Acidic Chloride Media Using Phosphonium-based Ionic Liquid as an Anion Exchanger," *Industrial & Engineering Chemistry Research,* vol. 54, no. 4, pp. 1350-1358, 2015/02/04 2015, doi: 10.1021/ie5045742.

[59] C. Shen, R. Li, J. Pei, J. Cai, T. Liu, and Y. Li, "Preparation and the Effect of Surface-Functionalized Calcium Carbonate Nanoparticles on Asphalt Binder," *Applied Sciences,* vol. 10, no. 1, 2020, doi: 10.3390/app10010091.

[60] F. Ippolito, G. Hübner, T. Claypole, and P. Gane, "Influence of the Surface Modification of Calcium Carbonate on Polyamide 12 Composites," *Polymers,* vol. 12, no. 6, 2020, doi: 10.3390/polym12061295.

[61] J. M. MartÍN-MartÍNez, "Chapter 13 - Rubber base adhesives," in *Adhesion Science and Engineering*, D. A. Dillard, A. V. Pocius, and M. Chaudhury Eds. Amsterdam: Elsevier Science B.V., 2002, pp. 573-675.

[62] G. Wypych, "5 - PRINCIPLES OF UV DEGRADATION," in *PVC Degradation and Stabilization (Third Edition)*, G. Wypych Ed. Boston: ChemTec Publishing, 2015, pp. 167-203.

[63] S. K. Haldar, "Chapter 1 - Minerals and rocks," in *Introduction to Mineralogy and Petrology (Second Edition)*, S. K. Haldar Ed. Oxford: Elsevier, 2020, pp. 1-51.

[64] J. Camiletti, A. M. Soliman, and M. L. Nehdi, "Effects of nano- and micro-limestone addition on early-age properties of ultra-high-performance concrete," *Materials and Structures,* vol. 46, no. 6, pp. 881-898, 2013/06/01 2013, doi: 10.1617/s11527-012-9940-0.

[65] M. Ni and B. D. Ratner, "Differentiation of Calcium Carbonate Polymorphs by Surface Analysis Techniques - An XPS and TOF-SIMS study," (in eng), *Surf Interface Anal,* vol. 40, no. 10, pp. 1356-1361, 2008, doi: 10.1002/sia.2904.

[66] S. Grasby, "Naturally precipitating vaterite (μ-CaCO3) spheres: Unusual carbonates formed in an extreme environment," *Geochimica et Cosmochimica Acta,* vol. 67, pp. 1659-1666, 05/01 2003, doi: 10.1016/S0016-7037(00)01304-2.

[67] C.-q. Li *et al.*, "Surface modification of calcium carbonate: A review of theories, methods and applications," *Journal of Central South University,* vol. 28, no. 9, pp. 2589-2611, 2021/09/01 2021, doi: 10.1007/s11771-021-4795-6.

[68] K. Cho, H. Chang, D. S. Kil, B.-G. Kim, and H. D. Jang, "Synthesis of dispersed CaCO3 nanoparticles by the ultrafine grinding," *Journal of Industrial and Engineering Chemistry,* vol. 15, no. 2, pp. 243-246, 2009/03/01/ 2009, doi: https://doi.org/10.1016/j.jiec.2008.10.005.

[69] L. S. Gomez-Villalba, P. López-Arce, M. Alvarez de Buergo, and R. Fort, "Atomic Defects and Their Relationship to Aragonite–Calcite Transformation in Portlandite Nanocrystal Carbonation," *Crystal Growth & Design,* vol. 12, no. 10, pp. 4844-4852, 2012/10/03 2012, doi: 10.1021/cg300628m.

[70] M. A. Hubbe and R. A. Gill, "Fillers for Papermaking: A Review of their Properties, Usage Practices, and their Mechanistic Role," *2016,* Fillers; Minerals products; Calcium carbonate; PCC; Kaolin clay; Titanium dioxide vol. 11, no. 1, p. 78, 2016-02-02 2016. [Online]. Available: https://ojs.cnr.ncsu.edu/index.php/BioRes/article/view/BioRes_11_1_2886_Hubbe_Gill_Review_Fillers_Papermaking.

[71] S. El-Sherbiny, S. M. El-Sheikh, and A. Barhoum, "Preparation and modification of nano calcium carbonate filler from waste marble dust and commercial limestone for papermaking wet end application," *Powder Technology,* vol. 279, pp. 290-300, 2015/07/01/ 2015, doi: https://doi.org/10.1016/j.powtec.2015.04.006.

[72] B. Cioni and A. Lazzeri, "The Role of Interfacial Interactions in the Toughening of Precipitated Calcium Carbonate–Polypropylene Nanocomposites," *Composite Interfaces,* vol. 17, no. 5-7, pp. 533-549, 2010/01/01 2010, doi: 10.1163/092764410X513486.

[73] S. M. Cao, "Research on the Application of Limestone Powder in Concrete Engineering," *Applied Mechanics and Materials,* vol. 174-177, pp. 341-344, 2012, doi: 10.4028/www.scientific.net/AMM.174-177.341.

[74] D. K. Panesar, M. Aqel, D. Rhead, and H. Schell, "Effect of cement type and limestone particle size on the durability of steam cured self-consolidating concrete," *Cement and Concrete Composites,* vol. 80, pp. 175-189, 2017/07/01/ 2017, doi: https://doi.org/10.1016/j.cemconcomp.2017.03.007.

[75] H. S. Yang, Y. J. Che, and M. Zhang, "Effect of Nano-CaCO3/Limestone Powder Composite on the Early Age Cement Hydration Products," *Key Engineering Materials,* vol. 703, pp. 354-359, 2016, doi: 10.4028/www.scientific.net/KEM.703.354.

[76] A. H. Mikhlif, I. A. Al-Jumaily, and B. S. Al-Numan, "Mechanical Properties of Sustainable Concrete Using Local Limestone Powder as Partial Replacement of Cement," in *2019 12th International Conference on Developments in eSystems Engineering (DeSE)*, 7-10 Oct. 2019 2019, pp. 105-108, doi: 10.1109/DeSE.2019.00029.

[77] T. Meng, Y. Yu, and Z. Wang, "Effect of nano-CaCO3 slurry on the mechanical properties and micro-structure of concrete with and without fly ash," *Composites Part B: Engineering,* vol. 117, pp. 124-129, 2017/05/15/ 2017, doi: https://doi.org/10.1016/j.compositesb.2017.02.030.

[78] M. Cao, X. Ming, K. He, L. Li, and S. Shen, "Effect of Macro-, Micro- and Nano-Calcium Carbonate on Properties of Cementitious Composites—A Review," *Materials,* vol. 12, no. 5, 2019, doi: 10.3390/ma12050781.

[79] C. J. Grimes, T. Hardcastle, M. S. Manga, T. Mahmud, and D. W. York, "Calcium Carbonate Particle Formation through Precipitation in a Stagnant Bubble and a Bubble Column Reactor," *Crystal Growth & Design,* vol. 20, no. 8, pp. 5572-5582, 2020/08/05 2020, doi: 10.1021/acs.cgd.0c00741.

[80] D. Konopacka-Łyskawa, "Synthesis Methods and Favorable Conditions for Spherical Vaterite Precipitation: A Review," *Crystals,* vol. 9, no. 4, 2019, doi: 10.3390/cryst9040223.

[81] K. N. Islam *et al.*, "Facile Synthesis of Calcium Carbonate Nanoparticles from Cockle Shells," *Journal of Nanomaterials,* vol. 2012, p. 534010, 2012/09/05 2012, doi: 10.1155/2012/534010.

[82] T. Thriveni, J. W. Ahn, C. Ramakrishna, Y. J. Ahn, and C. Han, "Synthesis of nano precipitated calcium carbonate by using a carbonation process through a closed loop reactor," *Journal of the Korean Physical Society,* vol. 68, no. 1, pp. 131-137, 2016/01/01 2016, doi: 10.3938/jkps.68.131.

[83] T. Kimura and N. Koga, "Monohydrocalcite in Comparison with Hydrated Amorphous Calcium Carbonate: Precipitation Condition and Thermal Behavior," *Crystal Growth & Design,* vol. 11, no. 9, pp. 3877-3884, 2011/09/07 2011, doi: 10.1021/cg200412h.

[84] C. Wang, P. Xiao, J. Zhao, X. Zhao, Y. Liu, and Z. Wang, "Biomimetic synthesis of hydrophobic calcium carbonate nanoparticles via a carbonation route," *Powder Technology,* vol. 170, no. 1, pp. 31-35, 2006/11/30/ 2006, doi: https://doi.org/10.1016/j.powtec.2006.08.016.

[85] Y. Boyjoo, V. K. Pareek, and J. Liu, "Synthesis of micro and nano-sized calcium carbonate particles and their applications," *Journal of Materials Chemistry A,* Review vol. 2, no. 35, pp. 14270-14288, 2014, doi: 10.1039/c4ta02070g.

[86] C. Wang *et al.*, "Facile preparation of CaCO3 nanoparticles with self-dispersing properties in the presence of dodecyl dimethyl betaine," *Colloids and Surfaces A: Physicochemical and Engineering Aspects,* Article vol. 297, no. 1-3, pp. 179-182, 2007, doi: 10.1016/j.colsurfa.2006.10.045.

[87] A. Fujii, T. Maruyama, Y. Ohmukai, E. Kamio, T. Sotani, and H. Matsuyama, "Cross-linked DNA capsules templated on porous calcium carbonate microparticles," *Colloids and Surfaces A: Physicochemical and Engineering Aspects,* vol. 356, no. 1, pp. 126-133, 2010/03/05/ 2010, doi: https://doi.org/10.1016/j.colsurfa.2010.01.008.

[88] A. Gal, W. Habraken, D. Gur, P. Fratzl, S. Weiner, and L. Addadi, "Calcite Crystal Growth by a Solid-State Transformation of Stabilized Amorphous Calcium Carbonate Nanospheres in a Hydrogel," *Angewandte Chemie International Edition,* https://doi.org/10.1002/anie.201210329 vol. 52, no. 18, pp. 4867-4870, 2013/04/26 2013, doi: https://doi.org/10.1002/anie.201210329.

[89] Q. L. Ren, Q. Luo, and F. L. Wang, "Effect of Anionic Surfactant on Adsorption Properties of Nano Calcium Carbonate," *Solid State Phenomena,* vol. 281, pp. 830-835, 2018, doi: 10.4028/www.scientific.net/SSP.281.830.

[90] J. Kontrec, D. Kralj, L. Brečević, and G. Falini, "Influence of some polysaccharides on the production of calcium carbonate filler particles," *Journal of Crystal Growth,* vol. 310, no. 21, pp. 4554-4560, 2008/10/15/ 2008, doi: https://doi.org/10.1016/j.jcrysgro.2008.07.106.

[91] D. N. Au - Azulay and L. Au - Chai, "Calcium Carbonate Formation in the Presence of Biopolymeric Additives," *JoVE,* no. 147, p. e59638, 2019/05/14/ 2019, doi: doi:10.3791/59638.

[92] N. Chhim, C. Kharbachi, T. Neveux, C. Bouteleux, S. Teychené, and B. Biscans, "Inhibition of calcium carbonate crystal growth by organic additives using the constant composition method in conditions of recirculating cooling circuits," *Journal of Crystal Growth,* vol. 472, pp. 35-45, 2017/08/15/ 2017, doi: https://doi.org/10.1016/j.jcrysgro.2017.03.004.

[93] D. Chakraborty and S. K. Bhatia, "Formation and Aggregation of Polymorphs in Continuous Precipitation. 2. Kinetics of CaCO3 Precipitation," *Industrial & Engineering Chemistry Research,* vol. 35, no. 6, pp. 1995-2006, 1996/01/01 1996, doi: 10.1021/ie950402t.

[94] N. Wada, N. Horiuchi, M. Nakamura, T. Hiyama, A. Nagai, and K. Yamashita, "Effect of Poly(acrylic acid) and Polarization on the Controlled Crystallization of Calcium Carbonate on Single-Phase Calcite Substrates," *Crystal Growth & Design,* vol. 13, no. 7, pp. 2928-2937, 2013/07/03 2013, doi: 10.1021/cg400337m.

[95] G. Hadiko, Y. S. Han, M. Fuji, and M. Takahashi, "Influence of Inorganic Ion on the Synthesis of Hollow Calcium Carbonate," *Advanced Materials Research,* vol. 11-12, pp. 677-680, 2006, doi: 10.4028/www.scientific.net/AMR.11-12.677.

[96] J.-P. Andreassen, R. Beck, and M. Nergaard, "Biomimetic type morphologies of calcium carbonate grown in absence of additives," *Faraday Discussions,* 10.1039/C2FD20056B vol. 159, no. 0, pp. 247-261, 2012, doi: 10.1039/C2FD20056B.

[97] O. A. Jimoh, K. S. Ariffin, H. B. Hussin, and A. E. Temitope, "Synthesis of precipitated calcium carbonate: a review," *Carbonates and Evaporites,* vol. 33, no. 2, pp. 331-346, 2018/06/01 2018, doi: 10.1007/s13146-017-0341-x.

[98] Y. Zhao, S. Li, L. Yu, Y. Liu, X. Wang, and J. Jiao, "The preparation of calcium carbonate crystals regulated by mixed cationic/cationic surfactants," *Journal of Crystal Growth,* vol. 324, no. 1, pp. 278-283, 2011/06/01/ 2011, doi: https://doi.org/10.1016/j.jcrysgro.2011.03.052.

[99] S. Li, L. Yu, F. Geng, L. Shi, L. Zheng, and S. Yuan, "Facile preparation of diversified patterns of calcium carbonate in the presence of DTAB," *Journal of Crystal Growth,* vol. 312, no. 10, pp. 1766-1773, 2010/05/01/ 2010, doi: https://doi.org/10.1016/j.jcrysgro.2010.02.019.

[100] H. Wei, Q. Shen, Y. Zhao, Y. Zhou, D. Wang, and D. Xu, "On the crystallization of calcium carbonate modulated by anionic surfactants," *Journal of Crystal Growth,* vol. 279, no. 3, pp. 439-446, 2005/06/01/ 2005, doi: https://doi.org/10.1016/j.jcrysgro.2005.02.064.

[101] Q. Zhang, L. Ren, Y. Sheng, Y. Ji, and J. Fu, "Control of morphologies and polymorphs of CaCO3 via multi-additives system," *Materials Chemistry and Physics,* vol. 122, no. 1, pp. 156-163, 2010/07/01/ 2010, doi: https://doi.org/10.1016/j.matchemphys.2010.02.053.

[102] M. Mihai, F. Bucătariu, M. Aflori, and S. Schwarz, "Synthesis and characterization of new CaCO3/poly(2-acrylamido-2-methylpropanesulfonic acid–co-acrylic acid) polymorphs, as templates for core/shell particles," *Journal of Crystal Growth,* vol. 351, no. 1, pp. 23-31, 2012/07/15/ 2012, doi: https://doi.org/10.1016/j.jcrysgro.2012.04.010.

[103] M. Lei, W. H. Tang, L. Z. Cao, P. G. Li, and J. G. Yu, "Effects of poly (sodium 4-styrene-sulfonate) on morphology of calcium carbonate particles," *Journal of Crystal Growth,* vol. 294, no. 2, pp. 358-366, 2006/09/04/ 2006, doi: https://doi.org/10.1016/j.jcrysgro.2006.06.029.

[104] M. Lei, W. H. Tang, and J. G. Yu, "Effect of a new functional double-hydrophilic block copolymer PAAL on the morphology of calcium carbonate particles," *Materials Research Bulletin,* vol. 40, no. 4, pp. 656-664, 2005/04/20/ 2005, doi: https://doi.org/10.1016/j.materresbull.2005.01.004.

[105] A.-J. Xie, Z.-W. Yuan, and Y.-h. Shen, "Biomimetic morphogenesis of calcium carbonate in the presence of a new amino-carboxyl-chelating-agent," *Journal of Crystal Growth,* vol. 276, no. 1, pp. 265-274, 2005/03/15/ 2005, doi: https://doi.org/10.1016/j.jcrysgro.2004.11.376.

[106] L. Zheng *et al.*, "Egg-white-mediated crystallization of calcium carbonate," *Journal of Crystal Growth,* vol. 361, pp. 217-224, 2012/12/15/ 2012, doi: https://doi.org/10.1016/j.jcrysgro.2012.09.003.

[107] B. Cheng, W. Cai, and J. Yu, "DNA-mediated morphosynthesis of calcium carbonate particles," *Journal of Colloid and Interface Science,* vol. 352, no. 1, pp. 43-49, 2010/12/01/ 2010, doi: https://doi.org/10.1016/j.jcis.2010.08.050.

[108] Z.-H. Xue, B.-B. Hu, X.-L. Jia, H.-W. Wang, and Z.-L. Du, "Effect of the interaction between bovine serum albumin Langmuir monolayer and calcite on the crystallization of CaCO3 nanoparticles," *Materials Chemistry and Physics,* vol. 114, no. 1, pp. 47-52, 2009/03/15/ 2009, doi: https://doi.org/10.1016/j.matchemphys.2008.07.002.

[109] X. Ji, G. Li, and X. Huang, "The synthesis of hollow CaCO3 microspheres in mixed solutions of surfactant and polymer," *Materials Letters,* vol. 62, no. 4, pp. 751-754, 2008/02/29/ 2008, doi: https://doi.org/10.1016/j.matlet.2007.06.063.

[110] L. Zhao and J. Wang, "Biomimetic synthesis of hollow microspheres of calcium carbonate crystals in the presence of polymer and surfactant," *Colloids and Surfaces A: Physicochemical and Engineering Aspects,* vol. 393, pp. 139-143, 2012/01/05/ 2012, doi: https://doi.org/10.1016/j.colsurfa.2011.11.012.

[111] G. W. Yan, J. H. Huang, J. F. Zhang, and C. J. Qian, "Aggregation of hollow CaCO3 spheres by calcite nanoflakes," *Materials Research Bulletin,* vol. 43, no. 8, pp. 2069-2077, 2008/08/04/ 2008, doi: https://doi.org/10.1016/j.materresbull.2007.09.014.

[112] K. Gorna, M. Hund, M. Vučak, F. Gröhn, and G. Wegner, "Amorphous calcium carbonate in form of spherical nanosized particles and its application as fillers for polymers," *Materials Science and Engineering: A,* vol. 477, no. 1, pp. 217-225, 2008/03/25/ 2008, doi: https://doi.org/10.1016/j.msea.2007.05.045.

[113] D. Konopacka-Łyskawa, B. Kościelska, and J. Karczewski, "Effect of some organic solvent–water mixtures composition on precipitated calcium carbonate in carbonation process," *Journal of Crystal Growth,* vol. 418, pp. 25-31, 2015/05/15/ 2015, doi: https://doi.org/10.1016/j.jcrysgro.2015.02.019.

[114] Y. Chen, X. Ji, G. Zhao, and X. Wang, "Facile preparation of cubic calcium carbonate nanoparticles with hydrophobic properties via a carbonation route," *Powder Technology,* vol. 200, no. 3, pp. 144-148, 2010/06/28/ 2010, doi: https://doi.org/10.1016/j.powtec.2010.02.017.

[115] L. Du, Y. Wang, and G. Luo, "In situ preparation of hydrophobic CaCO3 nanoparticles in a gas–liquid microdispersion process," *Particuology,* vol. 11, no. 4, pp. 421-427, 2013/08/01/ 2013, doi: https://doi.org/10.1016/j.partic.2012.07.009.

[116] W. Chuajiw, K. Takatori, T. Igarashi, H. Hara, and Y. Fukushima, "The influence of aliphatic amines, diamines, and amino acids on the polymorph of calcium carbonate precipitated by the introduction of carbon dioxide gas into calcium hydroxide aqueous suspensions," *Journal of Crystal Growth,* vol. 386, pp. 119-127, 2014/01/15/ 2014, doi: https://doi.org/10.1016/j.jcrysgro.2013.10.009.

[117] B.-C. Sun, X.-M. Wang, J.-M. Chen, G.-W. Chu, J.-F. Chen, and L. Shao, "Synthesis of nano-CaCO3 by simultaneous absorption of CO2 and NH3 into CaCl2 solution in a rotating packed bed," *Chemical Engineering Journal,* vol. 168, no. 2, pp. 731-736, 2011/04/01/ 2011, doi: https://doi.org/10.1016/j.cej.2011.01.068.

[118] S. Teir, T. Kotiranta, J. Pakarinen, and H.-P. Mattila, "Case study for production of calcium carbonate from carbon dioxide in flue gases and steelmaking slag," *Journal of CO2 Utilization,* vol. 14, pp. 37-46, 2016/06/01/ 2016, doi: https://doi.org/10.1016/j.jcou.2016.02.004.

[119] K. Song *et al.*, "Precipitation of calcium carbonate during direct aqueous carbonation of flue gas desulfurization gypsum," *Chemical Engineering Journal,* vol. 213, pp. 251-258, 2012/12/01/ 2012, doi: https://doi.org/10.1016/j.cej.2012.10.010.

[120] A. Alamdari, A. Alamdari, and D. Mowla, "Kinetics of calcium carbonate precipitation through CO2 absorption from flue gas into distiller waste of soda ash plant," *Journal of Industrial and Engineering Chemistry,* vol. 20, no. 5, pp. 3480-3486, 2014/09/25/ 2014, doi: https://doi.org/10.1016/j.jiec.2013.12.038.

[121] C. Zhang, J. Zhang, X. Feng, W. Li, Y. Zhao, and B. Han, "Influence of surfactants on the morphologies of CaCO3 by carbonation route with compressed CO2," *Colloids and Surfaces A: Physicochemical and Engineering Aspects,* vol. 324, no. 1, pp. 167-170, 2008/07/01/ 2008, doi: https://doi.org/10.1016/j.colsurfa.2008.04.010.

[122] Z. Namsaraev, A. Melnikova, A. Rudenko, and A. Komova, "Processes of Nanosized Calcium Carbonate Formation by Microorganisms," *Nanotechnologies in Russia,* vol. 15, pp. 20-27, 01/01 2020, doi: 10.1134/S199507802001005X.

[123] P. Bhutange Snigdha and M. V. Latkar, "Microbially Induced Calcium Carbonate Precipitation in Construction Materials," *Journal of Materials in Civil Engineering,* vol. 32, no. 5, p. 03120001, 2020/05/01 2020, doi: 10.1061/(ASCE)MT.1943-5533.0003141.

[124] H. Zhao, R. M. Dilmore, and S. N. Lvov, "Experimental studies and modeling of CO2 solubility in high temperature aqueous CaCl2, MgCl2, Na2SO4, and KCl solutions," *AIChE Journal,* https://doi.org/10.1002/aic.14825 vol. 61, no. 7, pp. 2286-2297, 2015/07/01 2015, doi: https://doi.org/10.1002/aic.14825.

[125] B. Liu, B. S. Mahmood, E. Mohammadian, A. Khaksar Manshad, N. R. Rosli, and M. Ostadhassan, "Measurement of Solubility of CO2 in NaCl, CaCl2, MgCl2 and MgCl2 + CaCl2 Brines at Temperatures from 298 to 373 K and Pressures up to 20 MPa Using the Potentiometric Titration Method," *Energies,* vol. 14, no. 21, 2021, doi: 10.3390/en14217222.

[126] B. P. Liu, J. Chen, F. B. Liu, S. B. Zhou, Y. D. Chen, and X. B. Huang, "Influence Factors of Calcium Carbonate Whiskers Prepared by Intermittent Bubbling Method," *Applied Mechanics and Materials,* vol. 310, pp. 80-84, 2013, doi: 10.4028/www.scientific.net/AMM.310.80.

[127] W. Wei *et al.*, "Preparation of Hierarchical Hollow CaCO3 Particles and the Application as Anticancer Drug Carrier," *Journal of the American Chemical Society,* vol. 130, no. 47, pp. 15808-15810, 2008/11/26 2008, doi: 10.1021/ja8039585.

[128] A. Chen, P. Ma, Z. Fu, Y. Wu, and W. Kong, "Crystallization and assembling behavior of calcium carbonate controlled by Ca-organic fibers," *Journal of Crystal Growth,* vol. 377, pp. 136-142, 2013/08/15/ 2013, doi: https://doi.org/10.1016/j.jcrysgro.2013.05.010.

[129] S. Ouhenia, D. Chateigner, M. A. Belkhir, E. Guilmeau, and C. Krauss, "Synthesis of calcium carbonate polymorphs in the presence of polyacrylic acid," *Journal of Crystal Growth,* vol. 310, no. 11, pp. 2832-2841, 2008/05/15/ 2008, doi: https://doi.org/10.1016/j.jcrysgro.2008.02.006.

[130] B. Feng, A. K. Yong, and H. An, "Effect of various factors on the particle size of calcium carbonate formed in a precipitation process," *Materials Science and Engineering: A,* vol. 445-446, pp. 170-179, 2007/02/15/ 2007, doi: https://doi.org/10.1016/j.msea.2006.09.010.

[131] J. Yu, M. Lei, B. Cheng, and X. Zhao, "Facile preparation of calcium carbonate particles with unusual morphologies by precipitation reaction," *Journal of Crystal Growth,* vol. 261, no. 4, pp. 566-570, 2004/02/01/ 2004, doi: https://doi.org/10.1016/j.jcrysgro.2003.09.035.

[132] B. Cheng, M. Lei, J. Yu, and X. Zhao, "Preparation of monodispersed cubic calcium carbonate particles via precipitation reaction," *Materials Letters,* vol. 58, no. 10, pp. 1565-1570, 2004/04/01/ 2004, doi: https://doi.org/10.1016/j.matlet.2003.10.027.

[133] Y. S. Han, G. Hadiko, M. Fuji, and M. Takahashi, "Factors affecting the phase and morphology of CaCO3 prepared by a bubbling method," *Journal of the European Ceramic Society,* vol. 26, no. 4, pp. 843-847, 2006/01/01/ 2006, doi: https://doi.org/10.1016/j.jeurceramsoc.2005.07.050.

[134] J. D. Rodriguez-Blanco, S. Shaw, P. Bots, T. Roncal-Herrero, and L. G. Benning, "The role of pH and Mg on the stability and crystallization of amorphous calcium carbonate," *Journal of Alloys and Compounds,* vol. 536, pp. S477-S479, 2012/09/25/ 2012, doi: https://doi.org/10.1016/j.jallcom.2011.11.057.

[135] Z. Chen and Z. Nan, "Controlling the polymorph and morphology of CaCO3 crystals using surfactant mixtures," *Journal of Colloid and Interface Science,* vol. 358, no. 2, pp. 416-422, 2011/06/15/ 2011, doi: https://doi.org/10.1016/j.jcis.2011.02.062.

[136] S. M. Song, J. H. Liu, and L. Wang, "Effects of Ultra-Fine Limestone Powder on Workability and Strength of High Strength Concrete," *Advanced Materials Research,* vol. 152-153, pp. 212-217, 2011, doi: 10.4028/www.scientific.net/AMR.152-153.212.

[137] M. Zajac, A. Rossberg, G. Le Saout, and B. Lothenbach, "Influence of limestone and anhydrite on the hydration of Portland cements," *Cement and Concrete Composites,* vol. 46, pp. 99-108, 2014/02/01/ 2014, doi: https://doi.org/10.1016/j.cemconcomp.2013.11.007.

[138] D. P. Bentz, C. F. Ferraris, S. Z. Jones, D. Lootens, and F. Zunino, "Limestone and silica powder replacements for cement: Early-age performance," *Cement and Concrete Composites,* vol. 78, pp. 43-56, 2017/04/01/ 2017, doi: https://doi.org/10.1016/j.cemconcomp.2017.01.001.

[139] Y. Ruan, T. Jamil, C. Hu, B. P. Gautam, and J. Yu, "Microstructure and mechanical properties of sustainable cementitious materials with ultra-high substitution level of calcined clay and limestone powder," *Construction and Building Materials,* vol. 314, p. 125416, 2022/01/03/ 2022, doi: https://doi.org/10.1016/j.conbuildmat.2021.125416.

[140] D. P. Bentz *et al.*, "Multi-scale investigation of the performance of limestone in concrete," *Construction and Building Materials,* vol. 75, pp. 1-10, 2015/01/30/ 2015, doi: https://doi.org/10.1016/j.conbuildmat.2014.10.042.

[141] V. Rahhal, V. Bonavetti, L. Trusilewicz, C. Pedrajas, and R. Talero, "Role of the filler on Portland cement hydration at early ages," *Construction and Building Materials,* vol. 27, no. 1, pp. 82-90, 2012/02/01/ 2012, doi: https://doi.org/10.1016/j.conbuildmat.2011.07.021.

[142] M. Cao, L. Xu, and C. Zhang, "Rheology, fiber distribution and mechanical properties of calcium carbonate (CaCO3) whisker reinforced cement mortar," *Composites Part A: Applied Science and Manufacturing,* vol. 90, pp. 662-669, 2016/11/01/ 2016, doi: https://doi.org/10.1016/j.compositesa.2016.08.033.

[143] K. Turk and M. L. Nehdi, "Coupled effects of limestone powder and high-volume fly ash on mechanical properties of ECC," *Construction and Building Materials,* vol. 164, pp. 185-192, 2018/03/10/ 2018, doi: https://doi.org/10.1016/j.conbuildmat.2017.12.186.

[144] J. Zhou, B. Yu, Y. Kong, W. Yang, and B. Cheng, "Effect of Limestone Powder on Mechanical Properties of Engineering Cementitious Composites," *Journal of Physics: Conference Series,* vol. 2076, no. 1, p. 012082, 2021/11/01 2021, doi: 10.1088/1742-6596/2076/1/012082.

[145] F. Sanchez and K. Sobolev, "Nanotechnology in concrete – A review," *Construction and Building Materials,* vol. 24, no. 11, pp. 2060-2071, 2010/11/01/ 2010, doi: https://doi.org/10.1016/j.conbuildmat.2010.03.014.

[146] J. Silvestre, N. Silvestre, and J. de Brito, "Review on concrete nanotechnology," *European Journal of Environmental and Civil Engineering,* vol. 20, no. 4, pp. 455-485, 2016/04/20 2016, doi: 10.1080/19648189.2015.1042070.

[147] D. Gao, L. Zhao, and G. Chen, "Flexural behavior of fiber and nanoparticle reinforced concrete at high temperatures," *Fire and Materials,* vol. 42, no. 7, pp. 725-740, 2018/11/01 2018, doi: 10.1002/fam.2526.

[148] N. Farzadnia, A. A. Abang Ali, and R. Demirboga, "Characterization of high strength mortars with nano alumina at elevated temperatures," *Cement and Concrete Research,* vol. 54, pp. 43-54, 2013/12/01/ 2013, doi: https://doi.org/10.1016/j.cemconres.2013.08.003.

[149] T. Sato and J. J. Beaudoin, "Effect of nano-CaCO3 on hydration of cement containing supplementary cementitious materials," *Advances in Cement Research,* vol. 23, no. 1, pp. 33-43, 2011, doi: 10.1680/adcr.9.00016.

[150] T. Sato and F. Diallo, "Seeding Effect of Nano-CaCO3 on the Hydration of Tricalcium Silicate," *Transportation Research Record,* vol. 2141, no. 1, pp. 61-67, 2010/01/01 2010, doi: 10.3141/2141-11.

[151] Z. Wu, C. Shi, K. H. Khayat, and S. Wan, "Effects of different nanomaterials on hardening and performance of ultra-high strength concrete (UHSC)," *Cement and Concrete Composites,* vol. 70, pp. 24-34, 2016/07/01/ 2016, doi: https://doi.org/10.1016/j.cemconcomp.2016.03.003.

[152] S. Yeşilmen, Y. Al-Najjar, M. H. Balav, M. Şahmaran, G. Yıldırım, and M. Lachemi, "Nano-modification to improve the ductility of cementitious composites," *Cement and Concrete Research,* vol. 76, pp. 170-179, 2015/10/01/ 2015, doi: https://doi.org/10.1016/j.cemconres.2015.05.026.

[153] J. Camiletti, A. M. Soliman, and M. L. Nehdi, "Effect of nano-calcium carbonate on early-age properties of ultra-high-performance concrete," *Magazine of Concrete Research,* vol. 65, no. 5, pp. 297-307, 2013, doi: 10.1680/macr.12.00015.

[154] D. Wang, C. Shi, Z. Wu, L. Wu, S. Xiang, and X. Pan, "Effects of nanomaterials on hardening of cement–silica fume–fly ash-based ultra-high-strength concrete," *Advances in Cement Research,* vol. 28, no. 9, pp. 555-566, 2016, doi: 10.1680/jadcr.15.00080.

[155] Z. Ge, K. Wang, R. Sun, D. Huang, and Y. Hu, "Properties of self-consolidating concrete containing nano-CaCO3," *Journal of Sustainable Cement-Based Materials,* vol. 3, no. 3-4, pp. 191-200, 2014/10/02 2014, doi: 10.1080/21650373.2014.903213.

[156] H. Yang, Y. Che, and F. Leng, "High volume fly ash mortar containing nano-calcium carbonate as a sustainable cementitious material: microstructure and strength development," *Scientific Reports,* vol. 8, no. 1, p. 16439, 2018/11/06 2018, doi: 10.1038/s41598-018-34851-4.

[157] A. Hosan, F. U. A. Shaikh, P. Sarker, and F. Aslani, "Nano- and micro-scale characterisation of interfacial transition zone (ITZ) of high volume slag and slag-fly ash blended concretes containing nano SiO2 and nano CaCO3," *Construction and Building Materials,* vol. 269, p. 121311, 2021/02/01/ 2021, doi: https://doi.org/10.1016/j.conbuildmat.2020.121311.

[158] EPA, "National Overview: Facts and Figures on Materials, Wastes and Recycling," ed, 2017.

[159] C. Lam, A. Ip, J. P. Barford, and G. McKay, "Use of Incineration MSW Ash: A Review," *Sustainability,* vol. 2, pp. 1943-1968, 2010.

[160] H. Luo, Y. Cheng, D. He, and E. Yang, "Review of leaching behavior of municipal sloid waste incineration (MSWI) ash," *Science of the Total Environment* vol. 668, pp. 90-103, 2019.

[161] X. Dou *et al.*, "Review of MSWI bottom ash utilization from perspectives of collective characterization, treatment and existing application," *Renewable and Sustainable Energy Reviews,* vol. 79, pp. 24-38, 2017.

[162] A. Joseph, R. Snelling, P. Van den Heede, S. Matthys, and N. De Belie, "The use of municipal solid waste incineration ash in various building materials: A Belgian point of view," *Materials,* vol. 11, p. 141, 2018.

[163] S. C. Gutiérrez-Gutiérrez, F. Coulon, Y. Jiang, and S. Wagland, "Rare earth elements and critical metal content of extracted landfilled material and potential recovery opportunities," *Waste Management,* vol. 42, pp. 128-136, 2015.

[164] YCSWA, "Ash Recycling and Processing Facility," ed: York County Solid Waste Authority 2019.

[165] Covanta, "Recycling Materials," ed: Covanta, 2019.

[166] J. T. Powell, T. G. Townsend, and J. B. Zimmerman, "Estimates of solid waste disposal rates and reduction targets for landfill gas emissions," *Nature Climate Change,* vol. 6, pp. 162-165, 2016.

[167] R. Kikuchi, "Recycling of municipal solid waste for cement production: pilot-scale test for transforming incineration ash of solid waste into cement clinker," *Resources, Conservation and Recycling,* vol. 31, no. 2, pp. 137-147, 2001.

[168] K. Wu, H. Shi, and X. Guo, "Utilization of municipal solid waste incineration fly ash for sulfoaluminate cement clinker production," *Waste Management,* vol. 31, pp. 2001-2008, 2011.

[169] K. O. Ampadu and K. Torii, "Characterization of ecocement pastes and mortars produced from incinerated ashes," *Cement and Concrete Research,* vol. 31, no. 3, pp. 431-436, 2001.

[170] J. E. Aubert, B. Husson, and A. Vaquier, "Use of municipal solid waste incineration fly ash in concrete," *Cement and Concrete Research,* vol. 34, no. 6, pp. 957-963, 2004/06/01/ 2004, doi: https://doi.org/10.1016/j.cemconres.2003.11.002.

[171] RUWI, "RUWI Process Overview," ed: Reuse Wastes Inc.

[172] T. Mangialardi, "Disposal of MSWI fly ash through a combined washing-immobilisation process," *Journal of Hazardous Materials,* vol. 98, no. 1-3, pp. 225-240, 2003.

[173] Y. Xiao, M. Oorsprong, Y. Yang, and J. Voncken, "Vitrification of bottom ash from a municipal solid waste incinerator," *Waste Management,* vol. 28, no. 6, pp. 1020-1026, 2008.

[174] K. A. Clavier, J. M. Paris, C. C. Ferraro, and T. G. Townsend, "Opportunities and challenges associated with using municipal waste incineration ash as a raw ingredient in cement production – a review," *Resources, Conservation & Recycling* vol. 160, p. 104888, 2020.

[175] L. M. Sarmiento, K. A. Clavier, J. M. Paris, C. C. Ferraro, and T. G. Townsend, "Critical examination of recycled municipal solid waste incineration ash as a mineral source for portland cement manufacture – A case study," *Resources, Conservation & Recycling,* vol. 148, pp. 1-10, 2019.

[176] P. Zhang, W. Liao, Q. Zhang, A. Kumar, and H. Ma, "Characterization of Sugarcane Bagasse Ash as a Potential Supplementary Cementitious Material: Comparison with Coal Combustion Fly Ash," *Journal of Cleaner Production,* vol. In Press, 2020.

[177] M. Alshaaer, B. El-Eswed, R. I. Yousef, F. Khalili, and H. Rahier, "Development of functional geopolymers for water purification, and construction purposes," *Journal of Saudi Chemical Society,* vol. 20, no. S1, pp. S85-S92, 2016.

[178] S. Robinson, "The Dangers of "Wishcycling"," in *Waste Management*, ed, 2018.

[179] NOAA. "Trends in atmospheric carbon dioxide." National Oceanic and Atmospheric Administration. https://gml.noaa.gov/ccgg/trends/global.html (accessed 10/10, 2021).

[180] EPA, "Facts and Figures about Materials, Waste and Recycling," 2019. [Online]. Available: https://www.epa.gov/facts-and-figures-about-materials-waste-and-recycling/guide-facts-and-figures-report-about#Materials.

[181] B. H. Cho, B. H. Nam, J. An, and H. Youn, "Municipal Solid Waste Incineration (MSWI) Ashes as Construction Materials—A Review," *Materials,* vol. 13, no. 14, p. 3143, 2020. [Online]. Available: https://www.mdpi.com/1996-1944/13/14/3143.

[182] J. T. Powell, T. G. Townsend, and J. B. Zimmerman, "Estimates of solid waste disposal rates and reduction targets for landfill gas emissions," *Nature Climate Change,* vol. 6, no. 2, pp. 162-165, 2016/02/01 2016, doi: 10.1038/nclimate2804.

[183] H. Long *et al.*, "Assessment of popular techniques for co-processing municipal solid waste in Chinese cement kilns," *Frontiers of Environmental Science & Engineering,* vol. 16, no. 4, p. 51, 2021/09/13 2021, doi: 10.1007/s11783-021-1485-4.

[184] B. Wang and C. Fan, "Hydration behavior and immobilization mechanism of MgO–SiO2–H2O cementitious system blended with MSWI fly ash," *Chemosphere,* vol. 250, p. 126269, 2020/07/01/ 2020, doi: https://doi.org/10.1016/j.chemosphere.2020.126269.

[185] Y. Zhang *et al.*, "Treatment of municipal solid waste incineration fly ash: State-of-the-art technologies and future perspectives," *Journal of Hazardous Materials,* vol. 411, p. 125132, 2021/06/05/ 2021, doi: https://doi.org/10.1016/j.jhazmat.2021.125132.

[186] E. R. Council, *The 2018 ERC Directory of Waste-to-Energy Facilities,* 2018. Energy Recovery Council: Washington, DC, USA,.

[187] F. Hasselriis, "Waste-to-Energy Ash Management in the United States," in *Renewable Energy Systems*, M. Kaltschmitt, N. J. Themelis, L. Y. Bronicki, L. Söder, and L. A. Vega Eds. New York, NY: Springer New York, 2013, pp. 1510-1531.

[188] W. Li *et al.*, "Evaluation of chemical speciation and environmental risk levels of heavy metals during varied acid corrosion conditions for raw and solidified/stabilized MSWI fly ash," *Waste Management,* vol. 87, pp. 407-416, 2019/03/15/ 2019, doi: https://doi.org/10.1016/j.wasman.2019.02.033.

[189] B. Guo *et al.*, "High-efficiency and low-carbon remediation of zinc contaminated sludge by magnesium oxysulfate cement," *Journal of Hazardous Materials,* vol. 408, p. 124486, 2021/04/15/ 2021, doi: https://doi.org/10.1016/j.jhazmat.2020.124486.

[190] C. H. K. Lam, A. W. M. Ip, J. P. Barford, and G. McKay, "Use of Incineration MSW Ash: A Review," *Sustainability,* vol. 2, no. 7, 2010, doi: 10.3390/su2071943.

[191] T. Sabbas *et al.*, "Management of municipal solid waste incineration residues," *Waste Management,* vol. 23, no. 1, pp. 61-88, 2003/01/01/ 2003, doi: https://doi.org/10.1016/S0956-053X(02)00161-7.

[192] B. H. Cho, B. H. Nam, J. An, and H. Youn, "Municipal Solid Waste Incineration (MSWI) Ashes as Construction Materials—A Review," *Materials,* vol. 13, no. 14, 2020, doi: 10.3390/ma13143143.

[193] J. Kim, B. H. Nam, B. A. A. Muhit, K. M. Tasneem, and J. An, "Effect of chemical treatment of MSWI bottom ash for its use in concrete," *Magazine of Concrete Research,* vol. 67, no. 4, pp. 179-186, 2015, doi: 10.1680/macr.14.00170.

[194] G. van der Wegen, U. Hofstra, and J. Speerstra, "Upgraded MSWI Bottom Ash as Aggregate in Concrete," *Waste and Biomass Valorization,* vol. 4, no. 4, pp. 737-743, 2013/12/01 2013, doi: 10.1007/s12649-013-9255-6.

[195] N. Czaplicka and D. Konopacka-Łyskawa, "Utilization of Gaseous Carbon Dioxide and Industrial Ca-Rich Waste for Calcium Carbonate Precipitation: A Review," *Energies,* vol. 13, no. 23, 2020, doi: 10.3390/en13236239.

[196] S. Heuss-Aßbichler, G. Magel, and K. T. Fehr, "Abiotic hydrogen production in fresh and altered MSWI-residues: Texture and microstructure investigation," *Waste Management,* vol. 30, no. 10, pp. 1871-1880, 2010/10/01/ 2010, doi: https://doi.org/10.1016/j.wasman.2010.02.015.

VITA

Bowen Tan, received his Bachelor of Engineering in June 2017) in Material Science and Technology from Southeast University, Nanjing, China. In May 2022, he received his master's degree in Civil Engineering from Missouri University of Science and Technology.